# OXIDE and SEMICONDUCTOR MAGNETISM

J. M. D. Coey

Physics Department, Trinity College, Dublin 2

Ireland.

1. Single-ion effects
2. Collective Effects
3. Examples

www.tcd.ie/Physics/Magnetism

Some references:

*Magnetic oxides*: D. J. Craik (editor) Wiley-Interscience 1975

*Magnetism and the chemical bond:* J. B. Goodenough Wiley-Interscience 1963

*Introduction to ligand field theory.* C. Ballhausen McGraw Hill 1962

*Mineralogical applications of crystal-field theory.* R. G. Burns CUP 1993 (2nd ed.)

*Point charge calculations of energy levels of magnetic ions in crystalline electric fields.* M. T. Hutchings Solid State Physics **16** 227 - 73 (1964)

# 1. Single-ion effects

1.1 Ubiquity of oxides. Oxide structures. Octahedral and tetrahedral sites. Magnetic ions – 3d, 4d, 4f.

1.2. Electronic structure of free ions (summary). Hund's rules. g-factors. Paramagnetic susceptibility.

1.3. Ions in solids. Crystal field. Crystal field Hamiltonian. One-electron states. 3d $t_{2g}$ and $e_g$ states. Notation. 2p-3d hybridization. One-electron energy-level diagrams in different symmetry. Quenching of orbital moment. Many-electron states. Orgel and Tanabe-Sugano diagrams.

1.4. Crystal field and anisotropy. Single-ion anisotropy. Determination of $B_n^m$.

# 1.1 Ubiquity of Oxides

Earth's crust is composed almost entirely of oxides — rocks, economic minerals, water.

Composition in **atomic** %

Oxygen ($O^{2-}$) is most abundant followed by silicon ($Si^{4+}$) and aluminium ($Al^{3+}$).

Crust is mostly composed of aluminosilicates.

Iron ($Fe^{2+}/Fe^{3+}$) is most abundant magnetic element. It is 40 times as abundant as all other magnetic elements together.

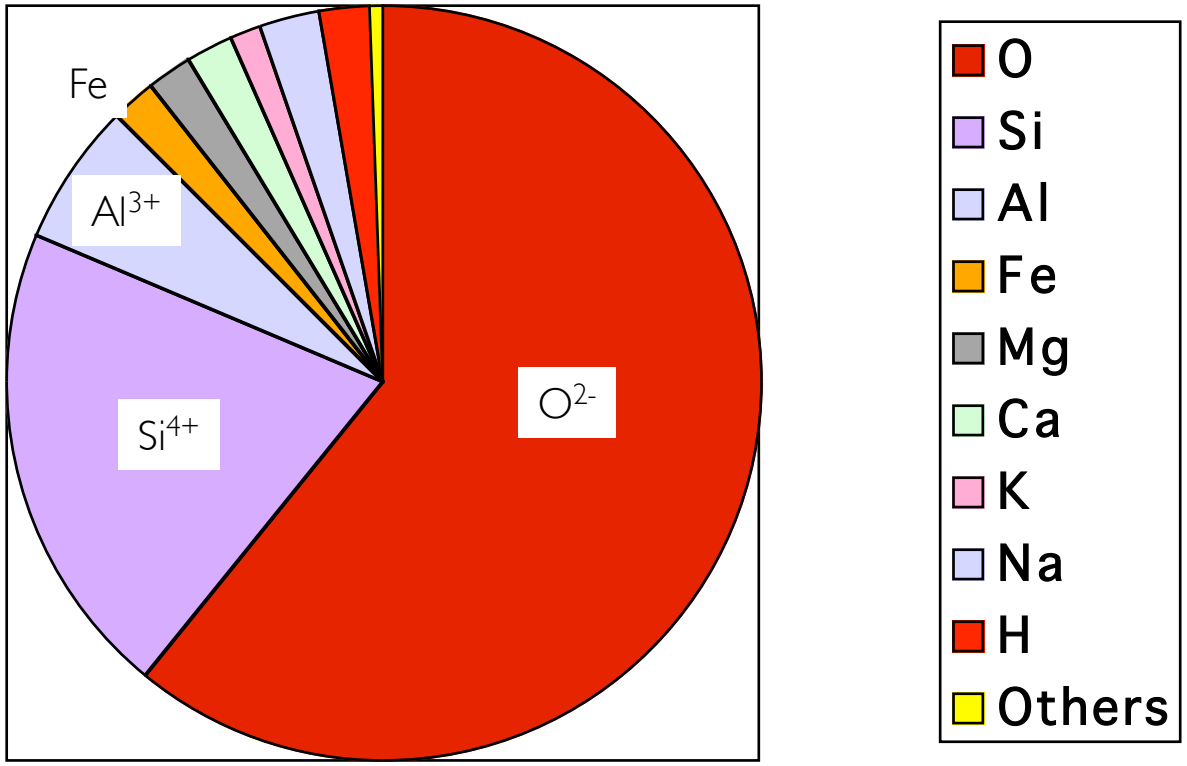

| Ion | Abundance (at%) | Configuration |
|---|---|---|
| $O^{2-}$ | 60.7 | $2p^6$ |
| $Si^{4+}$ | 20.6 | $2p^6$ |
| $Al^{3+}$ | 6.1 | $2p^6$ |
| $Na^{+}$ | 2.6 | $2p^6$ |
| $Fe^{2+/3+}$ | 2.1 | $3d^{6/5}$ |
| $H^{+}$ | 2.1 | $1s^0$ |
| $Ca^{2+}$ | 1.9 | $3p^6$ |
| $Mg^{2+}$ | 1.8 | $2p^6$ |
| $K^{+}$ | 1.5 | $3p^6$ |

Electronic configuration of 92% of the ions in the crust is the same $2p^6$ !

The $2p^6$ closed shell is very stable.

## Abundances of magnetic ions

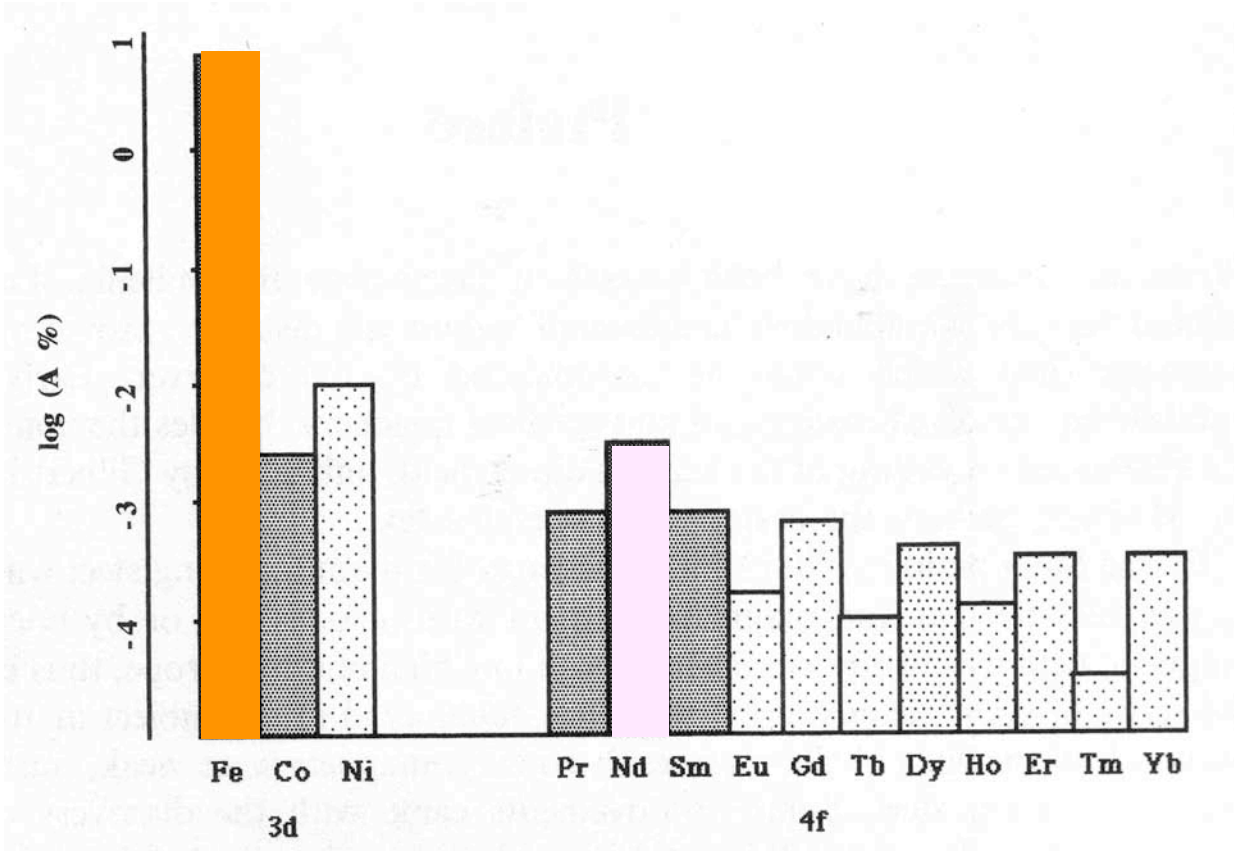


Price scales roughly inversely with abundance.

# Magnetic Periodic Table

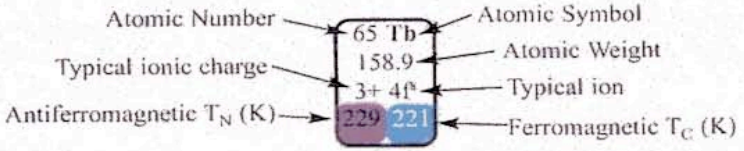


| | | | | | | | | | | | | | | | | | |
|---|---|---|---|---|---|---|---|---|---|---|---|---|---|---|---|---|---|
| 1 H 1.00 | | | | | | | | | | | | | | | | | 2 He 4.00 |
| 3 Li 6.94 1+ $2s^0$ | 4 Be 9.01 2+ $2s^0$ | | | | | | | | | | | 5 B 10.81 | 6 C 12.01 | 7 N 14.01 | 8 O 16.00 24 | 9 F 19.00 | 10 Ne 20.18 |
| 11 Na 22.99 1+ $3s^0$ | 12 Mg 24.21 2+ $3s^0$ | | | | | | | | | | | 13 Al 26.98 3+ $2p^6$ | 14 Si 28.09 | 15 P 30.97 | 16 S 32.07 | 17 Cl 35.45 | 18 Ar 39.95 |
| 19 K 39.10 1+ $4s^0$ | 20 Ca 40.08 2+ $4s^0$ | 21 Sc 44.96 3+ $3d^0$ | 22 Ti 47.88 4+ $3d^0$ | 23 V 50.94 4+ $3d^1$ | 24 Cr 52.00 3+ $3d^3$ 312 | 25 Mn 54.94 2+ $3d^5$ 96 | 26 Fe 55.85 3+ $3d^5$ 1043 | 27 Co 58.93 2+ $3d^7$ 1390 | 28 Ni 58.69 2+ $3d^8$ 629 | 29 Cu 63.55 2+ $3d^9$ | 30 Zn 65.39 2+ $3d^{10}$ | 31 Ga 69.72 3+ $3d^{10}$ | 32 Ge 72.61 | 33 As 74.92 | 34 Se 78.96 | 35 Br 79.90 | 36 Kr 83.80 |
| 37 Rb 85.47 1+ $5s^0$ | 38 Sr 87.62 2+ $5s^0$ | 39 Y 88.91 3+ $4d^0$ | 40 Zr 91.22 4+ $4d^0$ | 41 Nb 92.91 5+ $4d^0$ | 42 Mo 95.94 3+ $4d^3$ | 43 Tc 97.9 | 44 Ru 101.1 3+ $4d^5$ | 45 Rh 102.9 3+ $4d^6$ | 46 Pd 106.4 2+ $4d^8$ | 47 Ag 107.9 1+ $4d^{10}$ | 48 Cd 112.4 2+ $4d^{10}$ | 49 In 114.8 3+ $4d^{10}$ | 50 Sn 118.7 4+ $4d^{10}$ | 51 Sb 121.8 | 52 Te 127.6 | 53 I 126.9 | 54 Xe 131.6 |
| 55 Cs 132.9 1+ $6s^0$ | 56 Ba 137.3 2+ $6s^0$ | 57 La 138.9 3+ $4f^0$ | 72 Hf 178.5 4+ $5d^0$ | 73 Ta 180.9 5+ $5d^0$ | 74 W 183.8 6+ $5d^0$ | 75 Re 186.2 4+ $5d^3$ | 76 Os 190.2 3+ $5d^5$ | 77 Ir 192.2 4+ $5d^5$ | 78 Pt 195.1 2+ $5d^8$ | 79 Au 197.0 1+ $5d^{10}$ | 80 Hg 200.6 2+ $5d^{10}$ | 81 Tl 204.4 3+ $5d^{10}$ | 82 Pb 207.2 4+ $5d^{10}$ | 83 Bi 209.0 | 84 Po 209 | 85 At 210 | 86 Rn 222 |
| 87 Fr 223 | 88 Ra 226.0 2+ $7s^0$ | 89 Ac 227.0 3+ $5f^0$ | | | | | | | | | | | | | | | |

| | | | | | | | | | | | | | | |
|---|---|---|---|---|---|---|---|---|---|---|---|---|---|---|
| 58 Ce 140.1 3+ $4f^1$ 13 | 59 Pr 140.9 3+ $4f^2$ | 60 Nd 144.2 3+ $4f^3$ 19 | 61 Pm 145 | 62 Sm 150.4 3+ $4f^5$ 105 | 63 Eu 152.0 2+ $4f^7$ 90 | 64 Gd 157.3 3+ $4f^7$ 293 | 65 Tb 158.9 3+ $4f^8$ 229 221 | 66 Dy 162.5 3+ $4f^9$ 179 89 | 67 Ho 164.9 3+ $4f^{10}$ 132 20 | 68 Er 167.3 3+ $4f^{11}$ 85 20 | 69 Tm 168.9 3+ $4f^{12}$ 56 | 70 Yb 173.0 3+ $4f^{13}$ | 71 Lu 175.0 3+ $4f^{14}$ |
| 90 Th 232.0 4+ $5f^0$ | 91 Pa 231.0 5+ $5f^0$ | 92 U 238.0 4+ $5f^2$ | 93 Np 237.0 5+ $5f^2$ | 94 Pu 244 | 95 Am 243 | 96 Cm 247 | 97 Bk 247 | 98 Cf 251 | 99 Es 252 | 100 Fm 257 | 101 Md 258 | 102 No 259 | 103 Lr 260 | |

Ferromagnetic with $T_C$>290 K

Antiferromagnetic with $T_N$>290 K

Antiferromagnetic with $T_N$<290 K

Elements with ferromagnetic and antiferromagnetic transitions

Metals

Radioactive elements

# Ionic structures

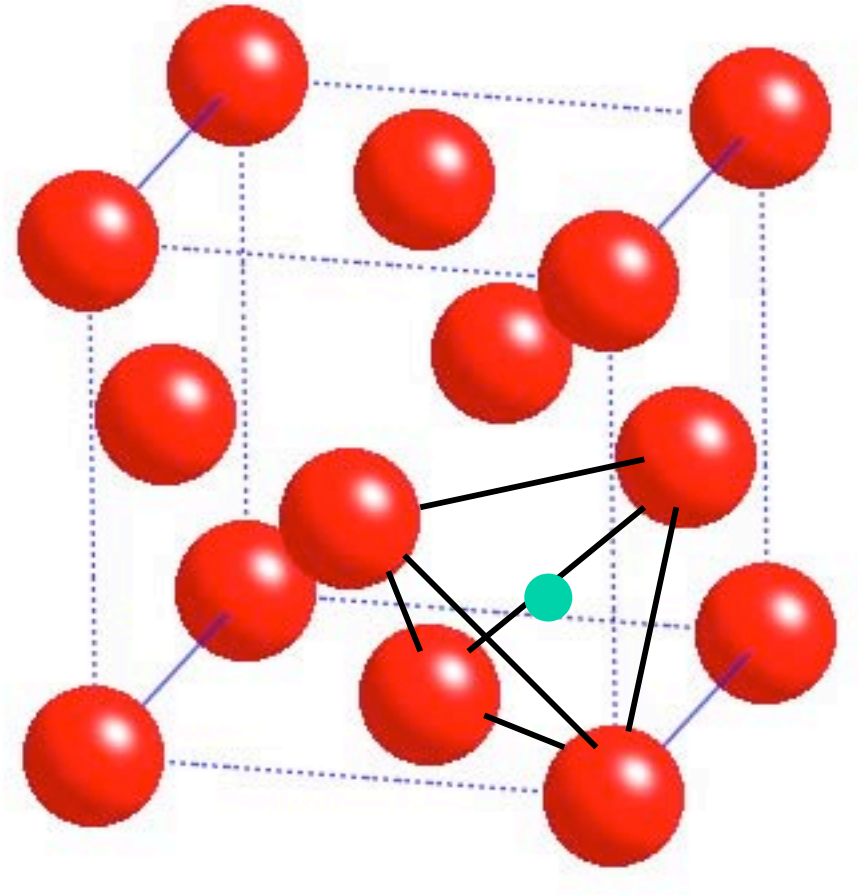

$R_{tet} = ((3/2)^{1/2} - 1)r_O = 0.32$ pm

Cation radii in oxides: low spin values are in parentheses.

| 4-fold tetrahedral | pm | 6-fold octahedral | pm | 6-fold octahedral | pm | 12-fold substitutional | pm |
|---|---|---|---|---|---|---|---|
| $Mg^{2+}$ | 53 | $Cr^{4+}$ $3d^2$ | 55 | $Ti^{3+}$ $3d^1$ | 67 | $Ca^{2+}$ | 134 |
| $Zn^{2+}$ | 60 | $Mn^{4+}$ $3d^3$ | 53 | $V^{3+}$ $3d^2$ | 64 | $Sr^{2+}$ | 144 |
| $Al^{3+}$ | 42 | | | $Cr^{3+}$ $3d^3$ | 62 | $Ba^{2+}$ | 161 |
| $Fe^{3+}$ $3d^5$ | 52 | $Mn^{2+}$ $3d^5$ | 83 | $Mn^{3+}$ $3d^4$ | 65 | $Pb^{2+}$ | 149 |
| | | $Fe^{2+}$ $3d^6$ | 78 (61) | $Fe^{3+}$ $3d^5$ | 64 | $Y^{3+}$ | 119 |
| | | $Co^{2+}$ $3d^7$ | 75 (65) | $Co^{3+}$ $3d^6$ | 61 (56) | $La^{3+}$ | 136 |
| | | $Ni^{2+}$ $3d^8$ | 69 | $Ni^{3+}$ $3d^7$ | 60 | $Gd^{3+}$ | 122 |

The radius of the $O^{2-}$ anion is 140 pm

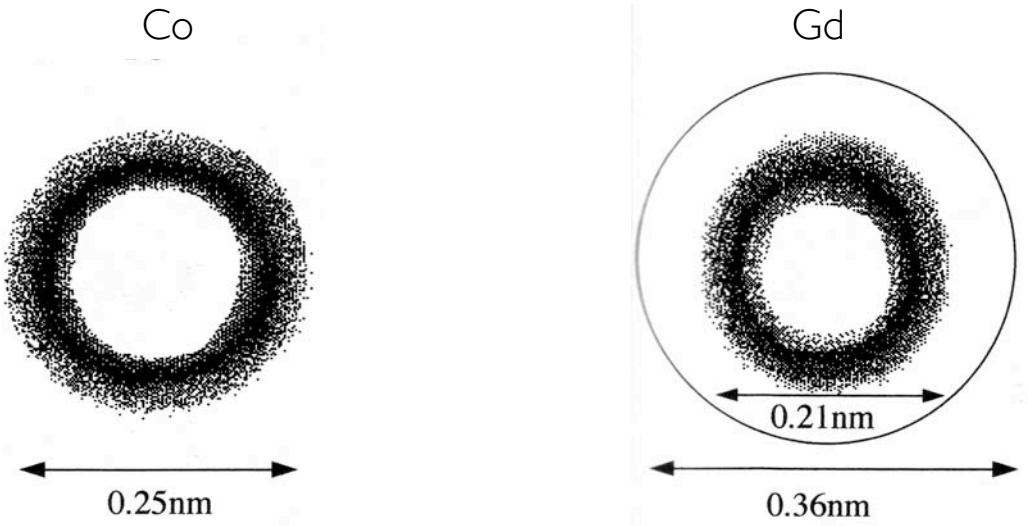


As metallic atoms, the transition metals occupy one third of the volume of the rare earths. As ions they occupy less than one tenth.

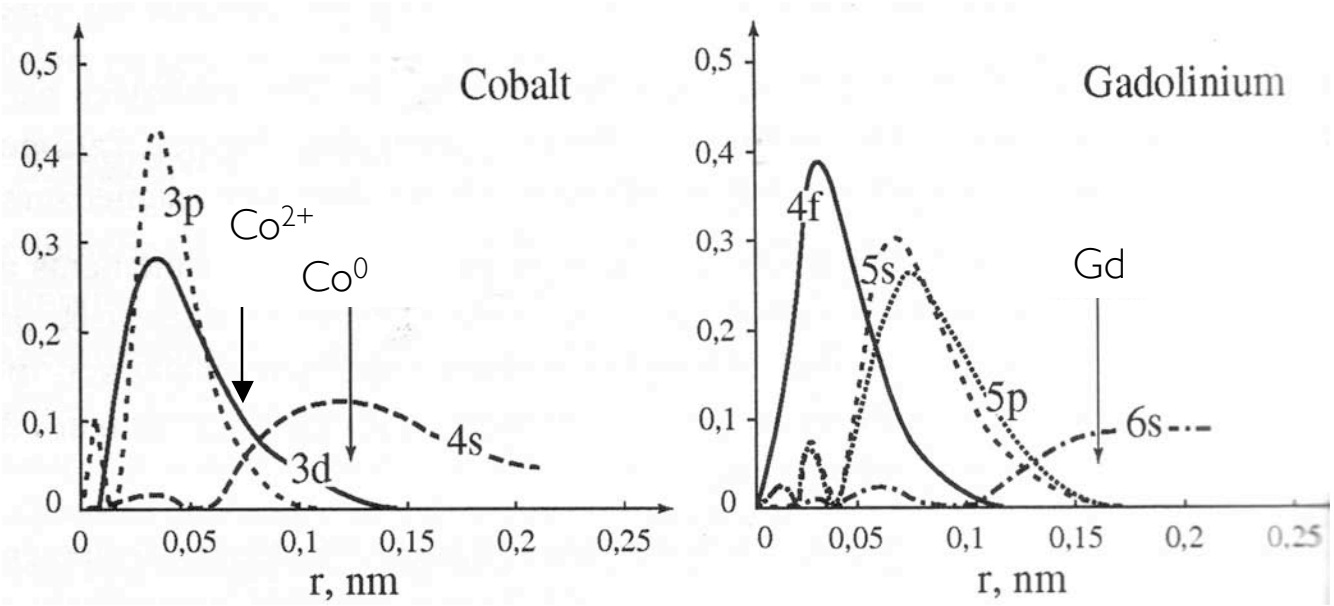

# 1.2 Electronic structure of free ions

Consider a *single electron* in a central potential. A hydrogenic atom is composed of a nucleus of charge Ze at the origin and an electron at r,□,□. First, consider a single electron in a central potential □$_e$ = Ze/4π□$_0$r

$$\mathcal{H} = -(\ddot{}^2/2m)\square^2 - Ze^2/4\pi\square_0 r$$

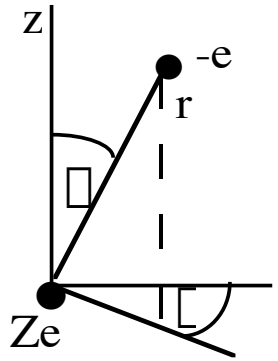


In polar coordinates:

$$\square^2 = \partial^2/\partial r^2 + (2/r)\partial/\partial r + 1/r^2\{\partial^2/\partial\square^2 + \cot\square\partial/\partial\square + (1/\sin^2\square)\partial^2/\partial^2\square\}$$

The term in parentheses is -ℓ$^2$. Schrödinger's equation is $\mathcal{H}\square = E\square$

The wave function □ means that the probability of finding the electron in a small volume dV ar **r** is □*(**r**)□(**r**)dV. (□* is the complex conjugate of □).

Eigenfunctions of the Schrödinger equation are of the form □(r,□,□) = R(r)□(□)□(□).

The angular part □(□)□(□) is written as $Y_l^{ml}$(□,□).

The *spherical harmonics* $Y_l^{ml}$(□,□) depend on two integers l, $m_l$, where l is ≥ 0 and $|m_l| \le l$.

□(□) = exp(i$m_l$□) where $m_l$ = 0, ±1, ±2 .....

The z-component of orbital angular momentum, represented by the operator ℓ$_z$ = -i¨∂/∂□, has eigenvalues <□ | ℓ$_z$ |□> = $m_l$¨.

□(□) = $P_l^{ml}$(cos□), are the associated Legendre polynomials with $l \ge |m_l|$, so $m_l$ = 0, ±1, ±2,....±l.

The square of the orbital angular momentum $\ell^2$ has eigenvalues $l(l+1)\hbar^2$. The orbital angular momentum has magnitude $[l(l+1)]^{1/2}\hbar$ and its projection along **z** can have any value from $-l\hbar$ to $+l\hbar$. The quantities $\ell_z$ and $\ell^2$ can be measured simultaneously (the operators commute). In the vector model, The total angular momentum is a vector which precesses around **z**.

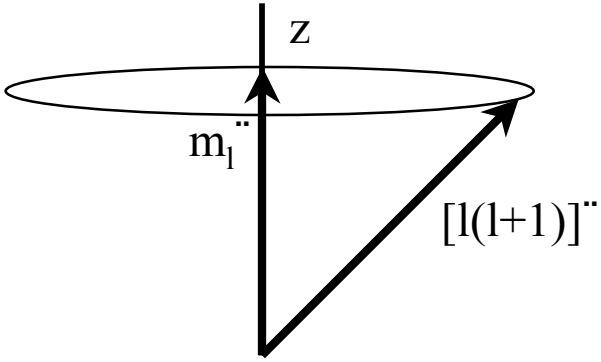


*Spherical harmonics*.

*s* $Y_0^0 = (1/4\pi)$

*p* $Y_1^0 = (3/4\pi)\cos\theta$ $Y_1^{\pm1} = \pm(3/8\pi)\sin\theta e^{\pm i\phi}$

*d* $Y_2^0 = (5/16\pi)(3\cos^2\theta - 1)$ $Y_2^{\pm1} = \pm(15/8\pi)\sin\theta\cos\theta e^{\pm i\phi}$
$Y_2^{\pm2} = (15/32\pi)\sin^2\theta e^{\pm2i\phi}$

*f* $Y_3^0 = (7/16\pi)(5\cos^3\theta - 3\cos\theta)$ $Y_3^{\pm1} = \pm(21/64\pi)(5\cos^2\theta - 1)\sin\theta e^{\pm i\phi}$
$Y_3^{\pm2} = (105/32\pi)\sin^2\theta\cos\theta e^{\pm2i\phi}$ $Y_3^{\pm3} = \pm(35/64\pi)\sin^3\theta e^{\pm3i\phi}$

- The radial part R(r) depends on l and also on n, the total quantum number; n > l; hence l = 0, 1, .....(n-1).

$$R(r) = V_n^l(Zr/na_0)\exp[-(Zr/na_0)]$$

$V_1^0 = 1$. Here $a_0 = 4\pi\varepsilon_0\hbar^2/me^2 = 52.9$ pm is the first *Bohr radius*, the basic length scale in atomic physics. The energy levels of the 1-electron atom are

$$E = -Zme^4/8h^2\varepsilon_0^2n^2 = -ZR/n^2$$

The quantity $R = me^4/8h^2\varepsilon_0 = 13.6$ eV is the Rydberg, the basic energy in atomic physics. For the central Coulomb potential $\varepsilon_e$, the potential energy V(r) depends only on r, not on $\theta$ or $\phi$. E depends only on n.

The three quantum numbers n, l, $m_l$ denote an *orbital*, a spatial distribution of electronic charge. Orbitals are denoted nx, x = s, p, d, f for l = 0, 1, 2, 3. Each orbital can accommodate up to two electrons with spin $m_s = \pm 1/2$. No two electrons can be in a state with the same four quantum numbers (Pauli exclusion principle). The hydrogenic orbitals are listed in the table

| | n | l | $m_l$ | $m_s$ | No of states |
|---|---|---|---|---|---|
| **1s** | **1** | **0** | **0** | **±1/2** | **2** |
| **2s** | **2** | **0** | **0** | **±1/2** | **2** |
| **2p** | **2** | **1** | **0,±1** | **±1/2** | **6** |
| **3s** | **3** | **0** | **0** | **±1/2** | **2** |
| **3p** | **3** | **1** | **0,±1** | **±1/2** | **6** |
| **3d** | **3** | **2** | **0,±1,±2** | **±1/2** | **10** |
| **4s** | **4** | **0** | **0** | **±1/2** | **2** |
| **4p** | **4** | **1** | **0,±1** | **±1/2** | **6** |
| **4d** | **4** | **2** | **0,±1,±2** | **±1/2** | **10** |
| **4f** | **4** | **3** | **0,±1,±2,±3** | **±1/2** | **14** |

- The Pauli principle states that no two electrons can have the same four quantum numbers. Each orbital can be occupied by at most two electrons with opposite spin.

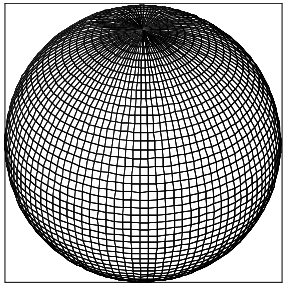

n =1
l = 0

s

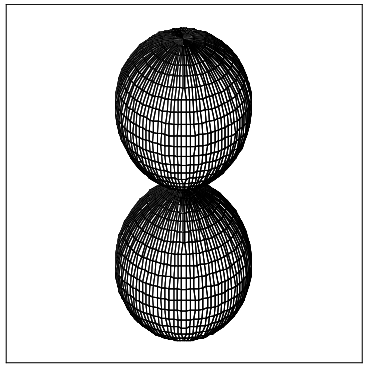

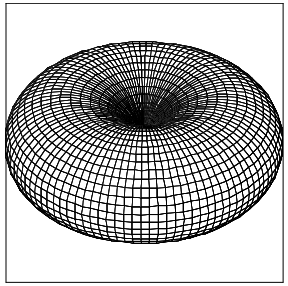

n =2
l = 1

p

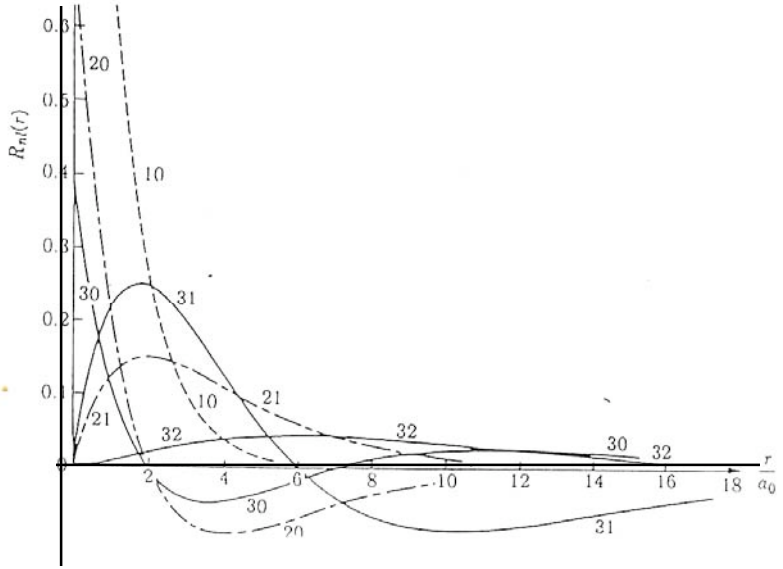


$m_l = 0$ $m_l = \pm 1$

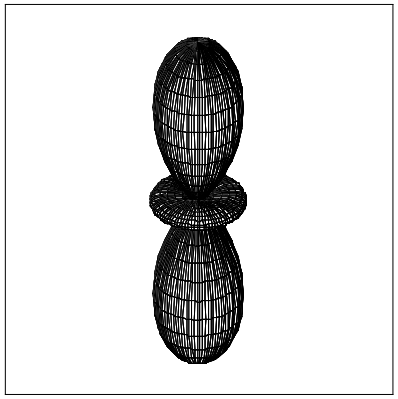

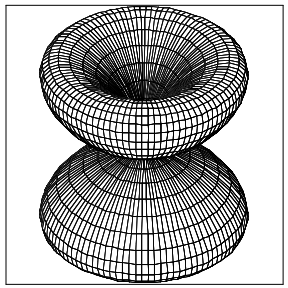

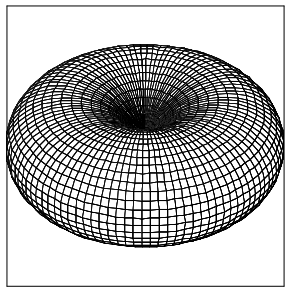

n =3
l = 2

d

$m_l = 0$ $m_l = \pm 1$ $m_l = \pm 2$

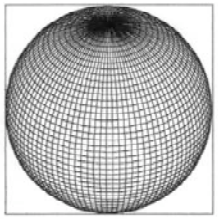

n =1
l = 0

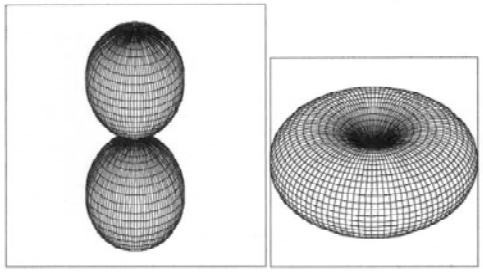

n =2
l = 1

$m_l = 0$ $m_l = \pm 1$

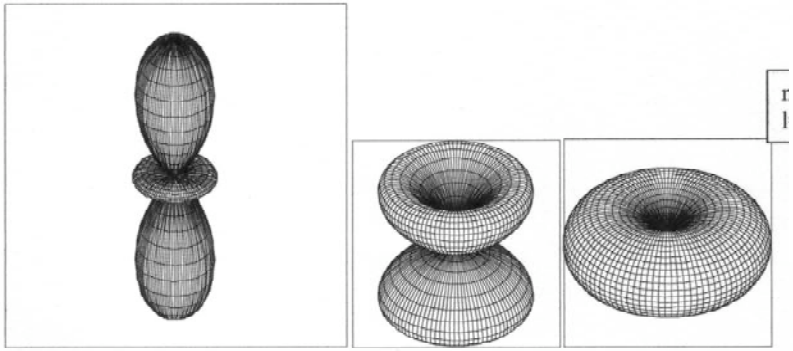

n =3
l = 2

## *The many-electron atom*.

In the many-electron atom, terms like $e^2/4\pi\varepsilon_0 r_{ij}$, must be added to the Hamiltonian. One way of dealing with the extra Coulomb interactions is to suppose that each electron sees a different spherical charge distribution, which produces a different central potential for each one. The potential with many electrons is not a simple Coulomb potential well; the degeneracy of electrons with different l is raised. The 4s shell, for example, is then lower in energy than the 3d shell, which defines the shape of the periodic table. The quantities $V_l(r)$ must be determined self-consistently (the Hartree-Foch approximation)

When several electrons are present on the same atom, at most two of them having opposite spin can occupy the same orbital (Pauli principle). Their spin and orbital angular momenta add to give resultants $S = \sum s_i$, $M_S = \sum m_{si}$, $L = \sum l_i$, $M_L = \sum m_{li}$.

Consider the six-electron carbon atom; $1s^2 2s^2 2p^2$. The 15 states fall into three groups, or *terms*.

The notation for terms is to denote L = 1. 2. 3. ….by S, P, D, …. and to include the spin multiplicity 2S + 1 as a superscript. The energy splitting of the terms is of order 1 eV.

$^{2S+1}L$

| 1s | 2s | 2p | $M_L$ | $M_S$ |
|---|---|---|---|---|
| ↑↓ | ↑↓ | ↑↓ | 2 | 0 |
| | | ↑ ↑ | 2 | 1 |
| | | ↑ ↓ | 1 | 0 |
| | | ↓ ↑ | 1 | 0 |
| | | ↓ ↓ | 1 | -1 |
| | | ↑ ↑ | 1 | 1 |
| | | ↑ ↓ | 0 | 0 |
| | | ↑↓ | 0 | 0 |
| | | ↓ ↑ | 0 | 0 |
| | | ↓ ↓ | 0 | -1 |
| | | ↓ ↑ | -1 | 0 |
| | | ↓ ↑ | -1 | 0 |
| | | ↑ ↑ | -1 | 1 |
| | | ↑↓ | -1 | 0 |

In spectroscopy, the energy unit $cm^{-1}$ is used. Handy conversions are: 1 eV ≡ 11605 K and 1 $cm^{-1}$ ≡ 1.44 K

| Term | L | S | $(M_L, M_S)$ |
|---|---|---|---|
| $^1S$ | 0 | 0 | (0,0) |
| $^3P$ | 1 | 1 | (1,1)(1,0)(1,-1)(0,1)(0,0)(0.-1)(-1,1)(-1,0)(-1,-1) |
| $^1D$ | 2 | 0 | (2,0)(1,0) (0,0)(-1,0)(-2,0) |

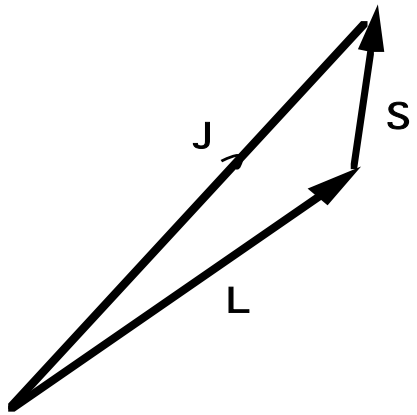


Addition of **L** and **S** in the vector model

Finally we need to couple the spin and orbital angular momentum to form a resultant J. $\mathbf{J} = \mathbf{L} + \mathbf{S}$

*Hund's rules*; A prescription for the lowest-energy state.

1) First maximize S for the configuration
2) Then maximize L consistent with that S
3) Finally couple L and S; J = L - S if shell is < half-full; J = L + S if shell is > half-full.

In the example, S = 1, L = 1, J = 0. The ground state of carbon is $^3P_0$, which is nonmagnetic (J = 0).
General notation for multiplets is $^{2S+1}X_J$ where X = S, P, D ..... for L = 0, 1, 2 .....

Some examples:

| | | | |
|---|---|---|---|
| $Fe^{3+}$ | $3d^5$ | ↑↑↑↑↑\| - - - - - | |
| S = 5/2 | L = 0 | J = 5/2 | $^6S_{5/2}$ |
| $Ni^{2+}$ | $3d^8$ | ↑↑↑↑↑\|□□□-- | |
| S = 1 | L = 3 | J = 4 | $^3F_4$ |
| $Nd^{3+}$ | $4f^3$ | ↑↑↑- - - - \|- - - - - - - | |
| S = 3/2 | L = 6 | J = 9/2 | $^4I_{9/2}$ |
| $Dy^{3+}$ | $4f^9$ | ↑↑↑↑↑↑↑\|□□- - - - - | |
| S = 5/2 | L = 5 | J = 15/2 | $^6H_{15/2}$ |

Variation of L, S, and J for the 3d and 4f series of atoms

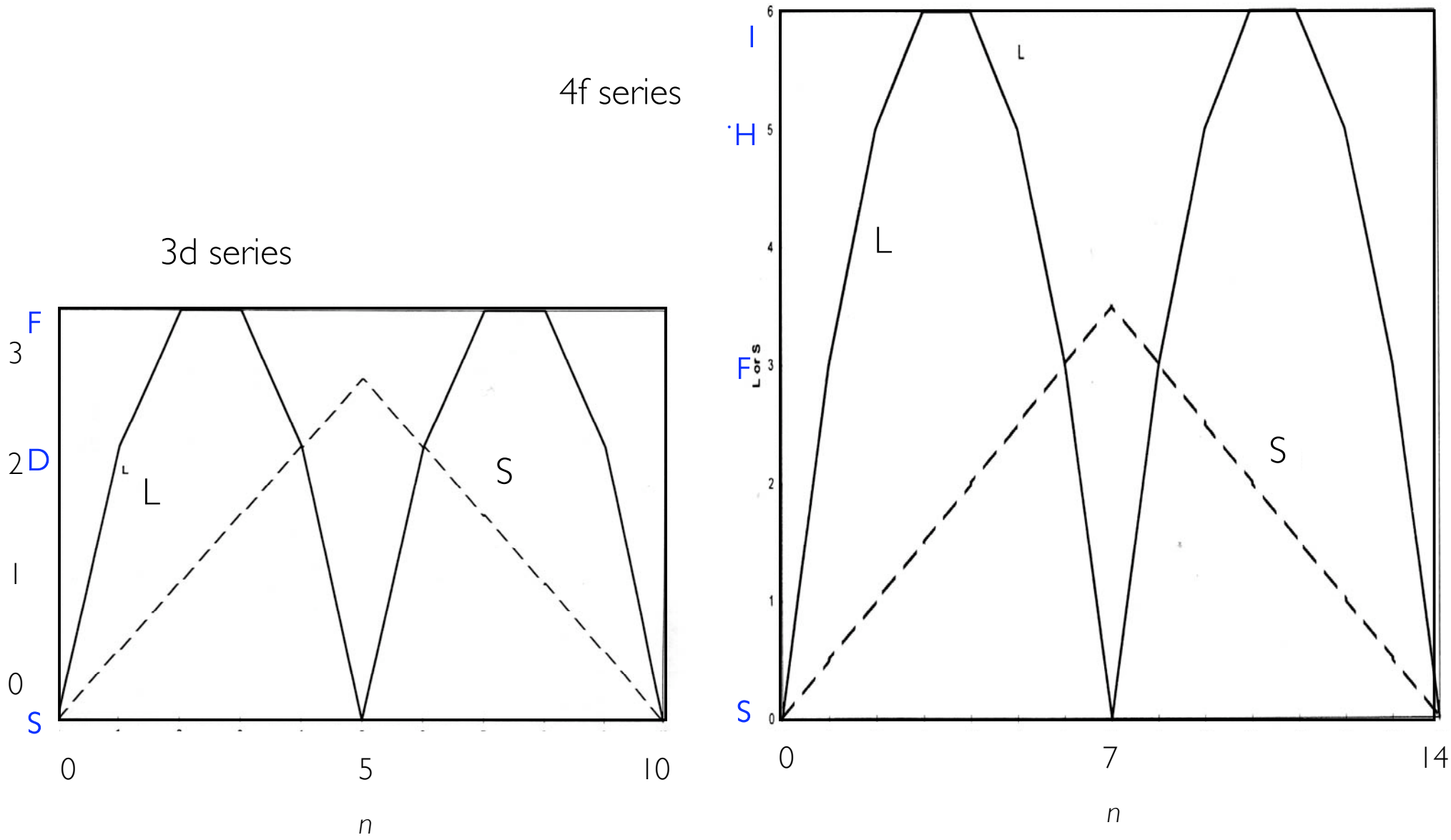

## *Spin-orbit coupling*

This relatively-weak relativistic interaction is responsible for Hund's third rule. In the multi-electron atom, the spin-orbit term in the Hamiltonian can be written as

$$\mathcal{H}_{so} = \zeta \mathbf{L.S}$$

$\zeta$ is $> 0$ for the first half of the 3d or 4f series and $< 0$ for the second half. It becomes large in heavy elements. $\zeta$ is related to the one-electron spin-orbit coupling constant $\lambda$ by $\zeta = \pm\lambda/2S$ for the first and second halves of the series. The resultant angular momentum (see above) is

$$\mathbf{J} = \mathbf{L} + \mathbf{S}$$

The identity $\mathbf{J}^2 = \mathbf{L}^2 + \mathbf{S}^2 + 2\,\mathbf{L.S}$ is used to evaluate $H_{so}$.The eigenvalues of $\mathbf{J}^2$ are $J(J+1)\ \ddot{}^2$ etc, hence $\mathbf{L.S}$ can be calculated.

*Spin-orbit coupling constants in the 3d and 4f series*

| | ion | $\zeta$ |
|---|---|---|
| $3d^1$ | $Ti^{3+}$ | 124 |
| $3d^2$ | $Ti^{2+}$ | 88 |
| $3d^3$ | $V^{2+}$ | 82 |
| $3d^4$ | $Cr^{2+}$ | 85 |
| $3d^6$ | $Fe^{2+}$ | -164 |
| $3d^7$ | $Co^{2+}$ | -272 |
| $3d^8$ | $Ni^{2+}$ | -493 |

| | | |
|---|---|---|
| $4f^1$ | $Ce^{3+}$ | 920 |
| $4f^2$ | $Pr^{3+}$ | 540 |
| $4f^3$ | $Nd^{3+}$ | 430 |
| $4f^5$ | $Sm^{3+}$ | 350 |
| $4f^8$ | $Tb^{3+}$ | -410 |
| $4f^9$ | $Dy^{3+}$ | -550 |
| $4f^{10}$ | $Ho^{3+}$ | -780 |
| $4f^{11}$ | $Er^{3+}$ | -1170 |
| $4f^{12}$ | $Tm^{3+}$ | -1900 |
| $4f^{13}$ | $Yb^{3+}$ | -4140 |

*Exercise:* Calculate the multiplet splitting in terms of $\zeta$, the spin-orbit interaction for an ion with L = 3, S = 1/2.

## Zeeman Interaction

The magnetic moment of an ion is represented by the term $\boldsymbol{m} = (\mathbf{L} + 2\mathbf{S})\mu_B/\ddot{}$
The Zeeman Hamiltonian for the magnetic moment in a field **B** applied along **z** is $-\boldsymbol{m}.\mathbf{B}$

$$\mathcal{H}_Z = (\mu_B/\ddot{})\mathbf{B}.(\mathbf{L} + 2\mathbf{S})$$

The vector model of the atom, including magnetic moments. First project ***m*** onto **J**. **J** then precesses around **z**.

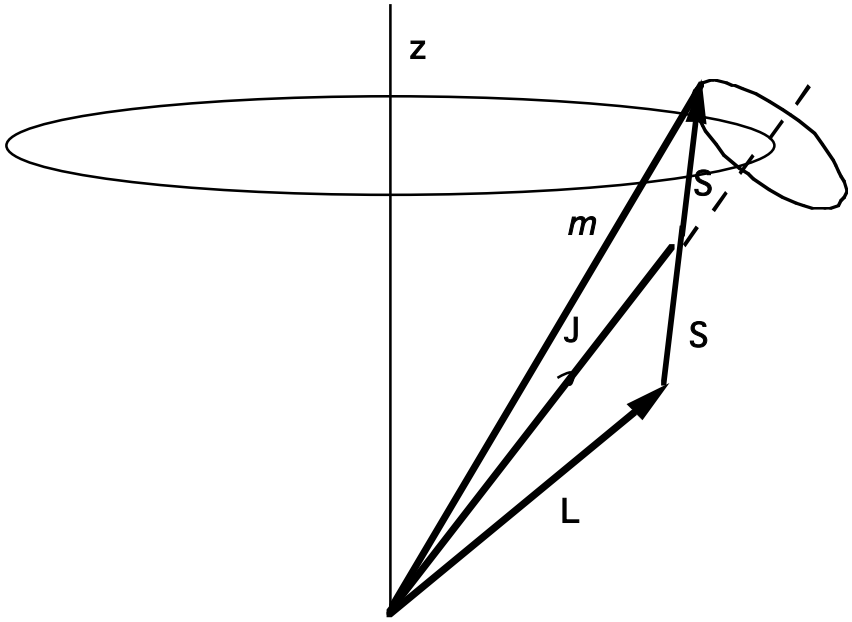


We define the g-factor for the atom or ion as the ratio of the component of magnetic moment along **J** in units of $\mu_B$ to the magnitude of the angular momentum in units of $\ddot{}$.

$g = -(\boldsymbol{m}.\mathbf{J}/\mu_B)/(\mathbf{J}^2/\ddot{}) = \boldsymbol{m}.\mathbf{J}/J(J+1)\ddot{}\mu_B.e$

but

$$\boldsymbol{m}.\boldsymbol{J} = (\mu_B/\ddot{})\{(\mathbf{L} + 2\mathbf{S}).(\mathbf{L} + \mathbf{S})\}$$
$$(\mu_B/\ddot{})\{(\mathbf{L}^2 + 3\mathbf{L}.\mathbf{S} + 2\mathbf{S}^2)\}$$
$$(\mu_B/\ddot{})\{(\mathbf{L}^2 + 2\mathbf{S}^2 + (3/2)(\mathbf{J}^2 - \mathbf{L}^2 - \mathbf{S}^2)\}$$
$$(\mu_B/\ddot{})\{((3/2)\mathbf{J}^2 - (1/2)\mathbf{L}^2 + (1/2)\mathbf{S}^2)\}$$
$$(\mu_B/\ddot{})\{((3/2)J(J+1) - (1/2)L(L+1) + (1/2)S(S+1)\}$$

$\mathbf{J}^2 = J(J+1)\ddot{}^2; \quad \mathbf{J}_z = M_J\ddot{}$

hence

$$g = 3/2 + \{S(S+1) - L(L+1)\}/2J(J+1)$$

Also, from the vector diagram it follows that $m_z/J_z = \mathbf{m.J}/\mathbf{J}^2 = g\mu_B/\ddot{}$.
The magnetic Zeeman energy is $E_Z = -m_z B$. This is $-(m_Z J_z)./(J_z B) = (g\mu_B/\ddot{})J_z B$

Hence $E_Z = -g\mu_B M_J B$

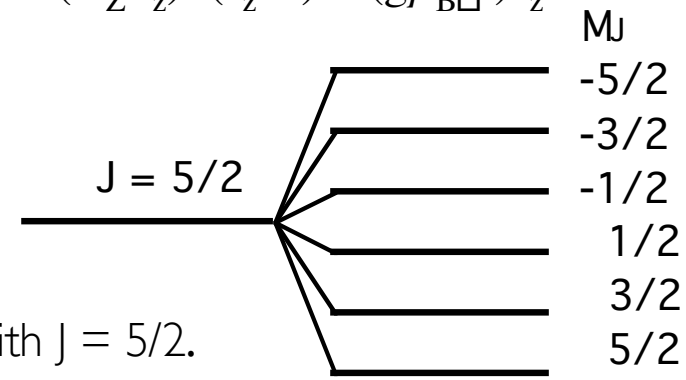


The effect of applying a magnetic field on an ion with J = 5/2.

Note the magnitudes of the energies involved: If g = 2. $\mu_B$ = 9.27 $10^{-24}$ J $T^{-1}$. The splitting of two adjacent energy levels is $g\mu_B B$. For B = 1 T, this is only $\approx 2\ 10^{-23}$ J, equivalent to 1.4 K. [$k_B = 1.38\ 10^{-23}$ J $K^{-1}$]

The basis of *electron spin resonance* is to apply a magnetic field to split the energy levels, and then apply radiation of frequency □ so that E = h□ is sufficient to induce transitions between the Zeeman levels. Since h = 6.63 $10^{-34}$ J $s^{-1}$, □ ≈ 28 GHz for resonance in 1 T. This is in the microwave range.

It is possible to deduce the total moment from the susceptibility, which should give $m_{eff} = g\ [J(J+1)]\mu_B$. for free ions. The maximum value of $m_z$ is deduced from the saturation magnetization. Generally $m_{eff} > m_z$

For 4f ions in so;ids J is the good quantum number, but for 3d ions S is the good quantum number

Energy levels of $Co^{2+}$ ion, $3d^7$. Note that the Zeeman splitting is not to scale.

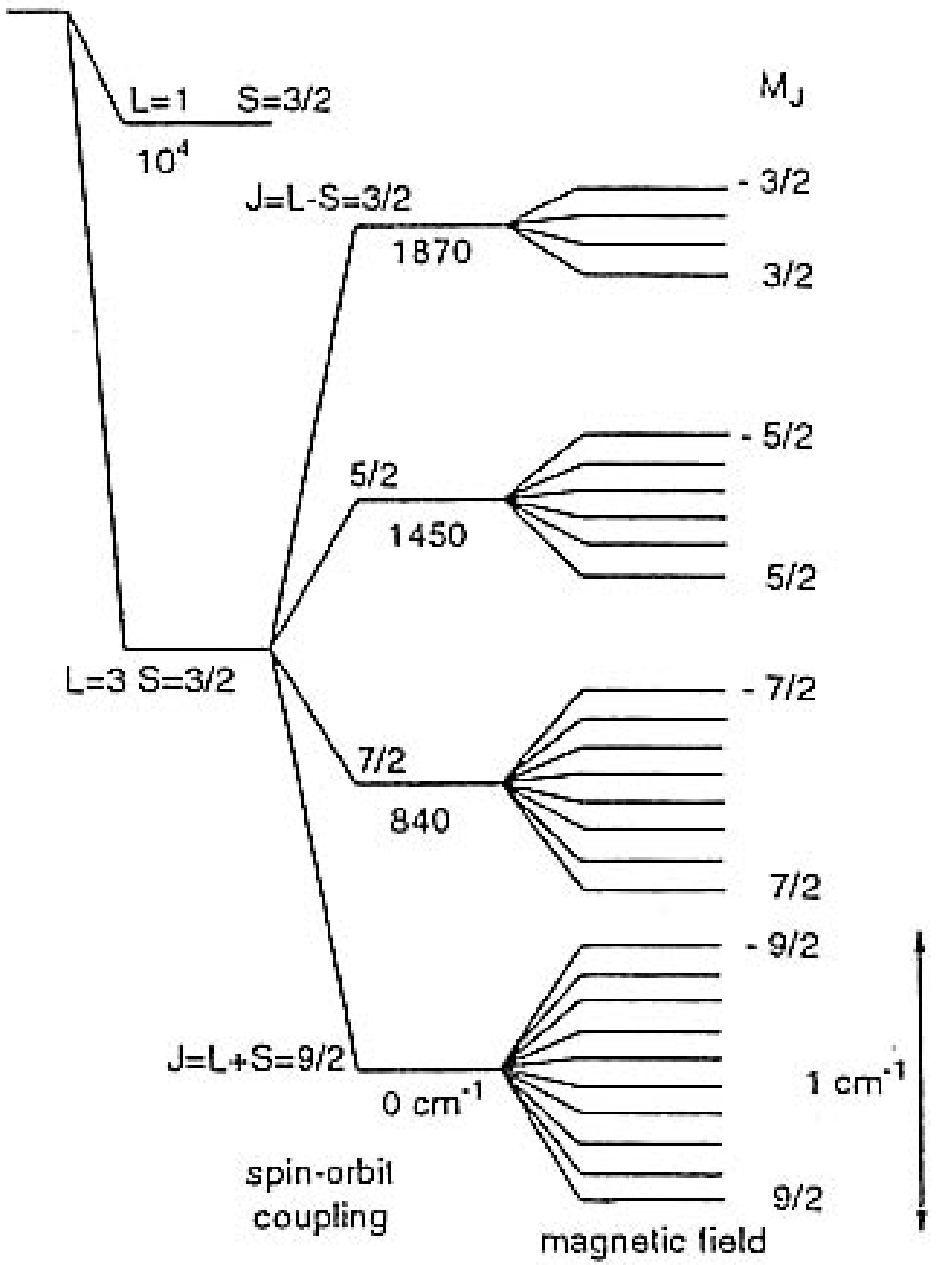

## *Paramagnetic Susceptibility*

The general quantum case was treated by *Brillouin*; $m$ is $g\mu_B J$, and x is defined as $x = \mu_0 mH/k_B T$. There are 2J+1 energy levels $E_i = -\mu_0 g\mu_B M_J H$, with moment $m_i = g\mu_B M_J$ where $M_J$ = J. J-1, J-2, … -J. The sums over the energy levels have 2J+1 terms. Their populations are proportional to $\exp(-E_i/kT)$

*a) Susceptibility* To calculate the susceptibility, we can take $x \ll 1$, because the susceptibility is defined as the initial slope of the magnetization curve. We expand the exponential as $\exp(x) = 1 + x + ..$,

$$\langle m \rangle = \sum_{-J}^{J} g\mu_B M_J (1 + \mu_0 g\mu_B M_J H/k_B T) / \sum_{-J}^{J} (1 + \mu_0 g\mu_B M_J H/k_B T)$$

Recall $\sum_{-J}^{J} 1 = 2J + 1$

$\sum_{-J}^{J} M_J = 0$

$\sum_{-J}^{J} M_J^2 = J(J + 1)(2J + 1)/3$

Hence $\langle m \rangle = \mu_0 g^2 \mu_B^2 HJ(J + 1)(2J + 1)/3(2J + 1)k_B T$

The relative susceptibility is N<m>/H, where N is the number of atoms/$m^3$.

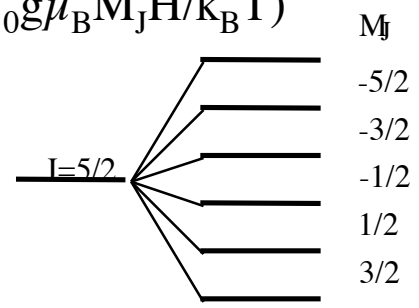


$$\chi_r = \mu_0 N g^2 \mu_B^2 J(J + 1)/3k_B T$$

This is the general form of the Curie law. Again it can be written $\chi_r = C/T$ where the *Curie constant* $C = \mu_0 N g^2 \mu_B^2 J(J+1)/3k_B$ or $C = \mu_0 N m_{eff}^2/3k_B$ where $m_{eff} = g\mu_B [J(J+1)]$. A typical value of $C$ for J = 1, N = $8.10^{28}$ $m^{-3}$ is 3.5 K. Note that results for the classical limit and S = 1/2 are obtained when J $\to \infty$ ($m = g\mu_B J$) and J = 1/2, g = 2. ($m = \mu_B$) .

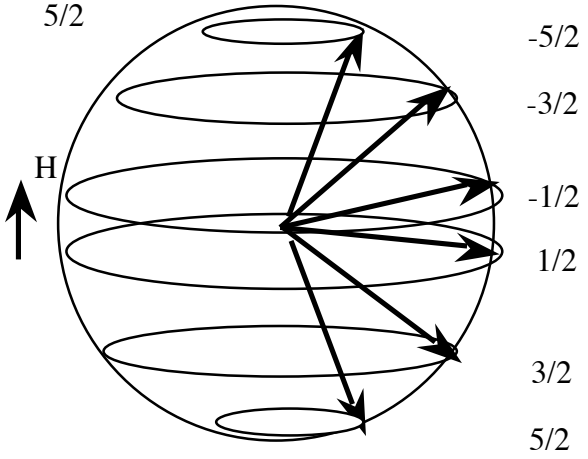

| Ion 3d | $^{2S+1}L_J$ | L | S | J | g | $m_{eff} = g\sqrt{J(J+1)}$ ($\mu_B$) | $m_s = 2\sqrt{S(S+1)}$ ($\mu_B$) | $m_{eff}^*$ ($\mu_B$) |
|---|---|---|---|---|---|---|---|---|
| $Ti^{2+}$, $V^{4+}$ ($3d^1$) | $^2D_{3/2}$ | 2 | 1/2 | 3/2 | 4/5 | 1.549 | 1.73 | 1.7 |
| $Ti^{2+}$, $V^{3+}$ ($3d^2$) | $^3F_2$ | 3 | 1 | 2 | 2/3 | 1.633 | 2.83 | 2.8 |
| $V^{2+}$, $Cr^{3+}$ ($3d^3$) | $^4F_{3/2}$ | 3 | 3/2 | 3/2 | 2/5 | 0.775 | 3.87 | 3.8 |
| $Cr^{2+}$, $Mn^{3+}$ ($3d^4$) | $^5D_0$ | 2 | 2 | 0 | - | - | 4.90 | 4.9 |
| $Mn^{2+}$, $Fe^{3+}$ ($3d^5$) | $^6S_{5/2}$ | 0 | 5/2 | 5/2 | 2 | 5.916 | 5.92 | 5.9 |
| $Fe^{2+}$, $Co^{3+}$ ($3d^6$) | $^5D_4$ | 2 | 2 | 4 | 3/2 | 6.708 | 4.90 | 5.4 |
| $Co^{2+}$, $Ni^{3+}$ ($3d^7$) | $^4F_{9/2}$ | 3 | 3/2 | 9/2 | 4/3 | 6.633 | 3.87 | 4.8 |
| $Ni^{2+}$ ($3d^8$) | $^3F_4$ | 3 | 1 | 4 | 5/4 | 5.590 | 2.83 | 3.2 |
| $Cu^{2+}$ ($3d^9$) | $^2D_{5/2}$ | 2 | 1/2 | 5/2 | 6/5 | 3.550 | 1.73 | 1.9 |

| Ion **4f** | $^{2S+1}L_J$ | L | S | J | g | $m_0=gJ$ ($\mu_B$) | $m_{eff}=g\sqrt{(J(J+1)}$ ($\mu_B$) | $m_{eff}$ ($\mu_B$) |
|---|---|---|---|---|---|---|---|---|
| **$Ce^{3+}$ ($4f^1$)** | **$^2F_{5/2}$** | **3** | **1/2** | **5/2** | **6/7** | **2.14** | **2.54** | **2.5** |
| **$P^{3+}$ ($4f^2$)** | **$^3H_4$** | **5** | **1** | **4** | **4/5** | **3.20** | **3.58** | **3.5** |
| **$Nd^{3+}$ ($4f^3$)** | **$^4I_{9/2}$** | **6** | **3/2** | **9/2** | **8/11** | **3.27** | **3.62** | **3.4** |
| **$Pm^{3+}$($4f^4$)** | **$^5I_4$** | **6** | **2** | **4** | **3/5** | **2.40** | **2.68** | **-** |
| **$Sm^{3+}$($4f^5$)** | **$^6H_{5/2}$** | **5** | **5/2** | **5/2** | **2/7** | **0.71** | **0.85** | **1.7** |
| **$Eu^{3+}$ ($4f^6$)** | **$^7F_0$** | **3** | **3** | **0** | **-** | **0.00** | **0.00** | **3.4** |
| **$Gd^{3+}$ ($4f^7$)** | **$^8S_{7/2}$** | **0** | **7/2** | **7/2** | **2** | **7.00** | **7.94** | **8.9** |
| **$Tb^{3+}$ ($4f^8$)** | **$^7F_6$** | **3** | **3** | **6** | **3/2** | **9.00** | **9.72** | **9.8** |
| **$Dy^{3+}$ ($4f^9$)** | **$^6H_{15/2}$** | **5** | **5/2** | **15/2** | **4/3** | **10.00** | **10.65** | **10.6** |
| **$Ho^{3+}$ ($4f^{10}$)** | **$^5I_8$** | **6** | **2** | **8** | **5/4** | **10.00** | **10.61** | **10.4** |
| **$Er^{3+}$ ($4f^{11}$)** | **$^4I_{15/2}$** | **6** | **3/2** | **15/2** | **6/5** | **9.00** | **9.58** | **9.5** |
| **$Tm^{3+}$ ($4f^{12}$)** | **$^3H_6$** | **5** | **1** | **6** | **7/6** | **7.00** | **7.56** | **7.6** |
| **$Yb^{3+}$ ($4f^{13}$)** | **$^2F_{7/2}$** | **3** | **1/2** | **7/2** | **8/7** | **4.00** | **4.53** | **4.5** |

## *Magnetization Curve*

To calculate the complete magnetization curve, set $y = \mu_0 g\mu_B H/k_B T$,

then $\langle m \rangle = g\mu_B \partial/\partial y[\ln \sum_{-J}^{J} \exp\{M_J y\}]$ $[d(\ln z)/dy = (1/z)\, dz/dy]$

The sum over the energy levels must be evaluated; it can be written as

$\exp(Jy)\{1 + r + r^2 + .....r^{2J}\}$ where $r = \exp\{-y\}$

The sum of a geometric progression $(1 + r + r^2 + .... + r^n) = (r^{n+1} - 1)/(r - 1)$

$\sum_{-J}^{J} \exp\{M_J y\} = (\exp\{-(2J+1)y\} - 1)\exp\{Jy\}/(\exp\{-y\}-1)$

multiply top and bottom by $\exp\{y/2\}$

$= [\sinh(2J+1)y/2]/[\sinh y/2]$

$\langle m \rangle = g\mu_B(\partial/\partial y)\ln\{[\sinh(2J+1)y/2]/[\sinh y/2]\}$

$= g\mu_B/2\,\{(2J+1)\coth(2J+1)y/2 - \coth y/2\}$

setting $x = Jy$, we obtain $\langle m \rangle = mB_J(x)$

where the Brillouin function $B_J(x) =$

$\{(2J+1)/2J\}\coth(2J+1)x/2J - (1/2J)\coth(x/2J)$.

Again, this reduces to the previous equations in the limits $J \to \infty$ ($m = g\mu_B J$) and $J = 1/2$, $g = 2$.

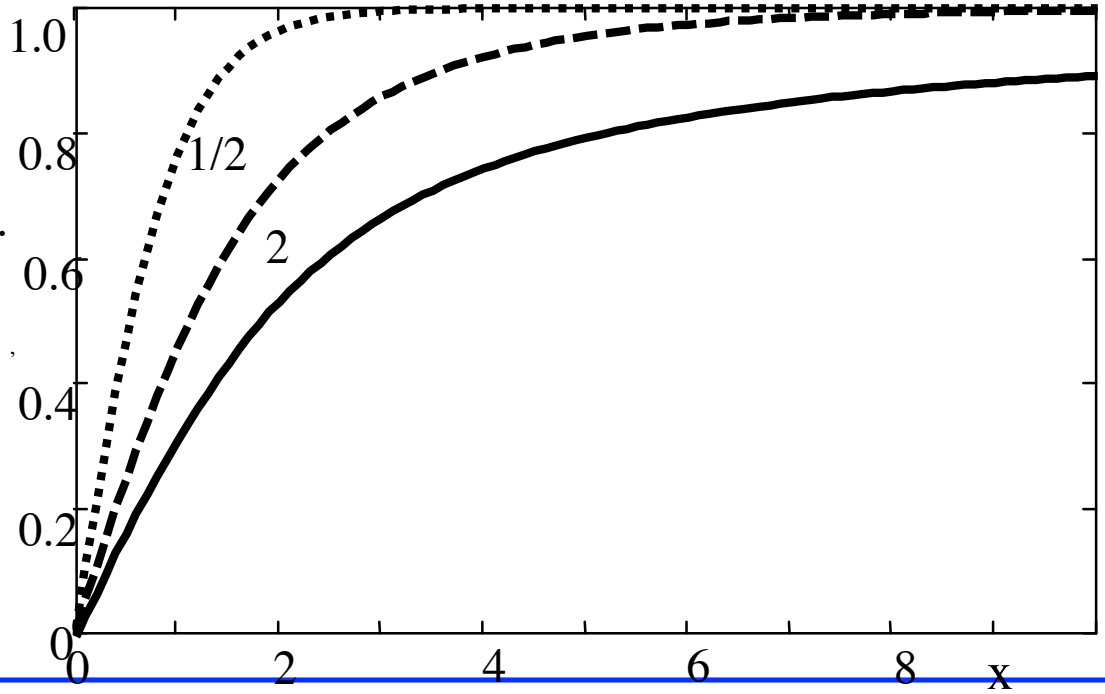


Comparison of the Langevin function and the Brillouin functions for J = 1/2 and J = 2.

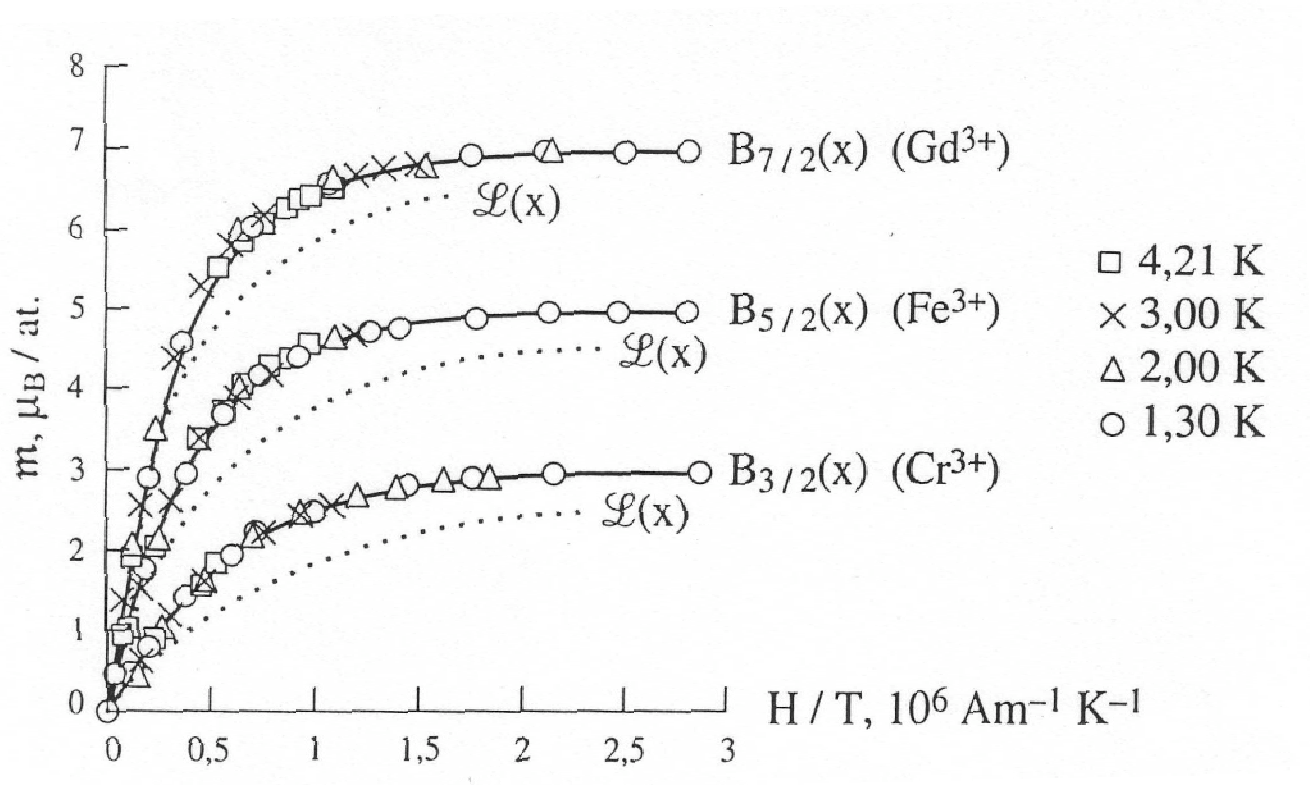


Reduced magnetization curves for three paramagnetic salts, with Brillouin-theory predictions

The theory of localized magnetism gives a good account of magnetically-dilute 3d and 4f salts where the magnetic moments do not interact with each other. Except in large fields or very low temperatures, the M(H) response is linear. Fields > 100 T would be needed to approach saturation at room temperature.

The excellence of the theory is illustrated by the fact that data for quite different temperatures superpose on a single Brillouin curve plotted as a function of $x \approx H/T$

# 1.3 Ions in Solids

Summarizing, for free ions;

Filled electronic shells are not magnetic (the spins are paired; $m_s = \pm 1/2$)

Only unfilled shells may possess a magnetic moment

The magnetic moment is given by $\boldsymbol{m} = g\mu_B \mathbf{J}$, where $\mathbf{J}$ represents the total angular momentum. For a given configuration the values of g and J in the ground state are given by Hund's rules

When the ion is embedded in a solid, the crystal field interaction is important, and the third point is modified

Orbital angular momentum for 3d ions is *quenched*. The spin only moment is $\boldsymbol{m} \approx g\mu_B \mathbf{S}$, with g = 2.

Magnetocrystalline anisotropy appears, making certain crystallographic axes easy directions of magnetization.

The Hamiltonian is now

$$\mathcal{H} = \mathcal{H}_0 + \mathcal{H}_{so} + \mathcal{H}_{cf} + \mathcal{H}_Z$$

Typical magnitudes of energy terms (in K)

| | $\mathcal{H}_0$ | $\mathcal{H}_{so}$ | $\mathcal{H}_{cf}$ | $\mathcal{H}_Z$ **in 1 T** |
|---|---|---|---|---|
| **3d** | **$1 - 5\ 10^4$** | **$10^2 - 10^3$** | **$1 - 10^4$** | **1** |
| **4f** | **$1 - 6\ 10^5$** | **$1 - 5\ 10^3$** | **$\approx 3\ 10^2$** | **1** |

$\mathcal{H}_{so}$ must be considered before $\mathcal{H}_{cf}$ for 4f ions, and the converse for 3d ions. Hence J is a good quantum number for 4f ions, but S is a good quantum number for 3d ions. The 4f electrons are generally localized, and 3d electrons are localized in oxides and other ionic compounds.

The most common coordination for 3d ions is 6-fold (octahedral) or 4-fold (tetrahedral). Both have cubic symmetry, if undistorted. The crystal field can be estimated from a point-charge sum.

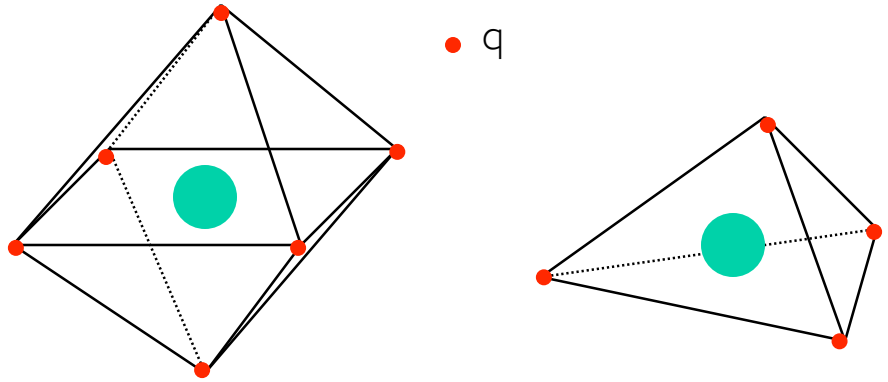


Octahedral and tetrahedral sites.

To demonstrate quenching of orbital angular momentum, we consider the l = 1 states $\psi^{0}, \psi^{1}, \psi^{-1}$ corresponding to $m_l = 0, \pm 1$.

$$\psi^{0} = R(r)\cos\theta$$
$$\psi^{\pm 1} = R(r)\sin\theta\exp\{\pm i\phi\}$$

The functions are eigenstates in the central potential V (r) but they are not eigenstates of $\mathcal{H}_{cf}$. Suppose the oxygens can be represented by point charges q at their centres, then for the octahedron,

$$\mathcal{H}_{cf} = eV_{cf} = Dq(x^4 + y^4 + z^4 - 3y^2z^2 - 3z^2x^2 - 3x^2y^2)$$

where $D \approx e/4\pi\varepsilon_0 a^6$. But $\psi^{\pm 1}$ are *not* eigenfunctions of $V_{cf}$, e.g. $\int \psi_i^{*} V_{cf} \psi^{j} dV \neq \psi_{ij}$, where i,j = -1, 0, 1.
We seek linear combinations that are eigenfunctions, namely

$$\psi^{0} = R(r)\cos\theta = zR(r) = p_z$$
$$(1/\sqrt{2})(\psi^{1} + \psi^{-1}) = R'(r)\sin\theta\cos\phi = xR(r) = p_x$$
$$(1/\sqrt{2})(\psi^{1} - \psi^{-1}) = R'(r)\sin\theta\sin\phi = yR(r) = p_y$$

Note that the z-component of angular momentum; $\mathbf{l}_z = i\hbar\partial/\partial\phi$ is *zero* for these wavefunctions. Hence the orbital angular momentum is quenched.

The same applies to 3d orbitals; the eigenfunctions there are

| | | | | |
|---|---|---|---|---|
| $d_{xy} = (1/\sqrt{2})(\Phi^2 - \Phi^{-2}) =$ | $R'(r)\sin^2\theta\sin2\phi$ | $\approx$ | $xyR(r)$ | |
| $d_{yz} = (1/\sqrt{2})(\Phi^1 - \Phi^{-1}) =$ | $R'(r)\sin\theta\cos\theta\sin\phi$ | $\approx$ | $yzR(r)$ | $t_{2g}$ *orbitals* |
| $d_{zx} = (1/\sqrt{2})(\Phi^1 + \Phi^{-1}) =$ | $R'(r)\sin\theta\cos\theta\cos\phi$ | $\approx$ | $zxR(r)$ | |
| $d_{x^2-y^2} = (1/\sqrt{2})(\Phi^2 + \Phi^{-2}) =$ | $R'(r)\sin^2\theta\cos2\phi$ | $\approx$ | $(x^2-y^2)R(r)$ | $e_g$ *orbitals* |
| $d_{3z^2-r^2} = \Phi^0 =$ | $R'(r)(3\cos^2\theta - 1)$ | $\approx$ | $(3z^2-r^2)R(r)$ | |

The three p-orbitals are degenerate in a cubic crystal field, whether octahedral or tetrahedral, whereas the five d-orbitals split into a group of three $t_{2g}$ and a group of two $e_g$ orbitals

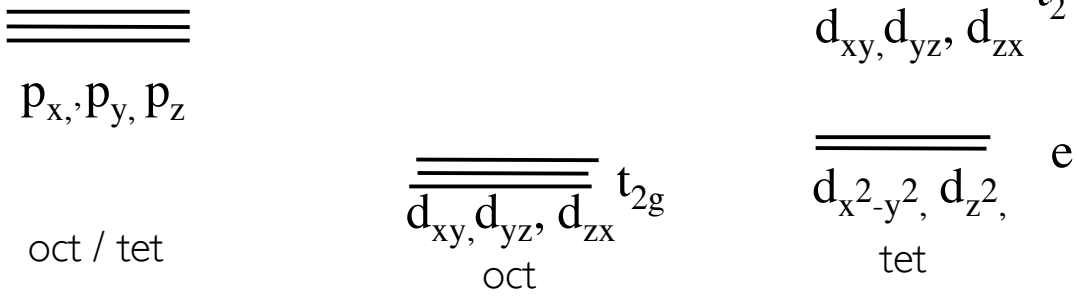


*Notation;* *a* or *b* denote a nondegenerate single-electron orbital, *e* a twofold degenerate orbital and *t* a threefold degenerate orbital. Capital letters refer to multi-electron states. *a*, *A* are nondegenerate and symmetric with respect to the principal axis of symmetry (the sign of the wavefunction is unchanged), *b*. *B* are antisymmetric with respect to the principal axis (the sign of the wavefunction changes). Subscripts *g* and *u* indicate whether the wavefunction is symmetric or antisymmetric under inversion. *1* refers to mirror planes parallel to a symmetry axis, *2* refers to diagonal mirror planes.

# Orbitals in the crystal field

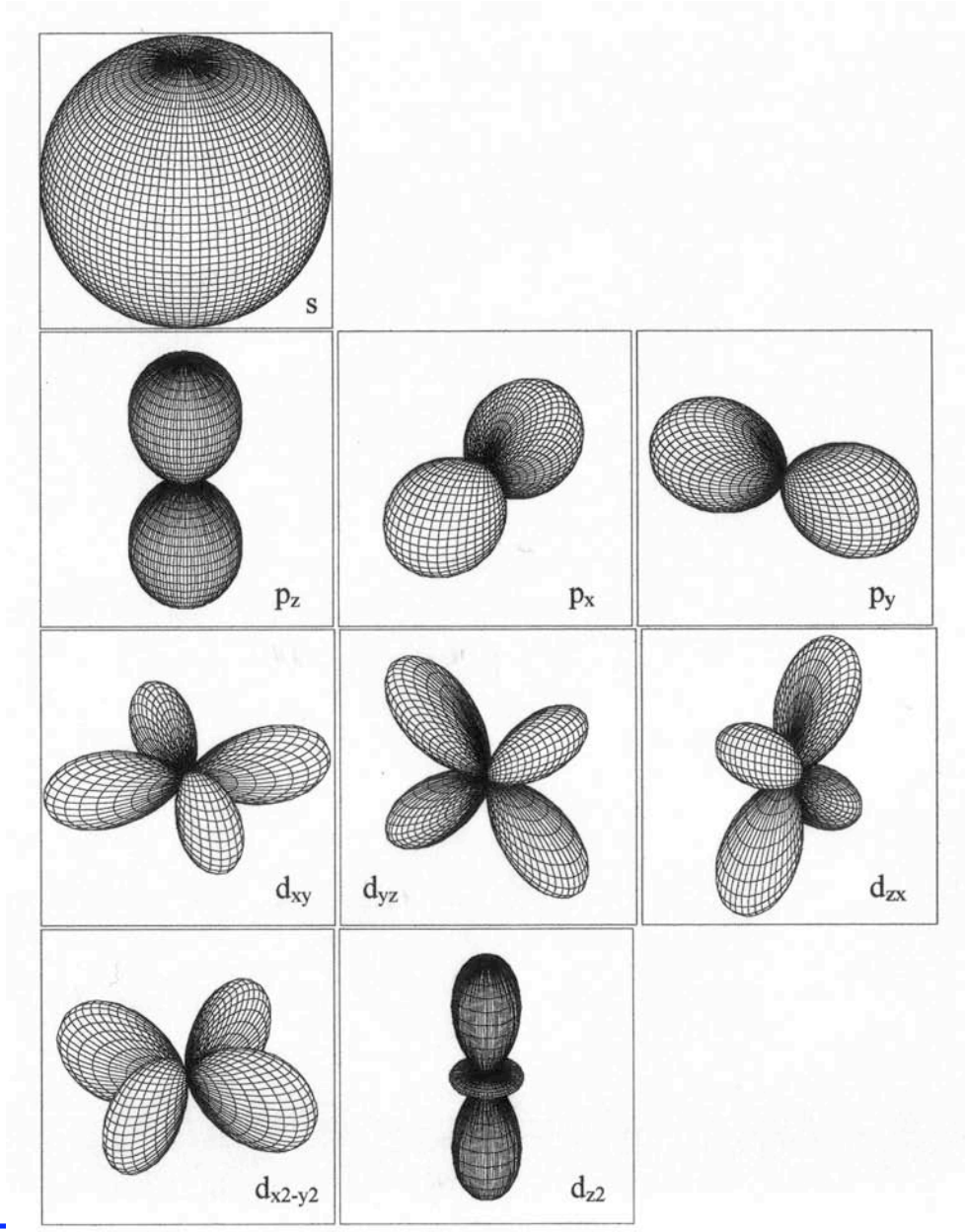

# One-electron energy diagrams

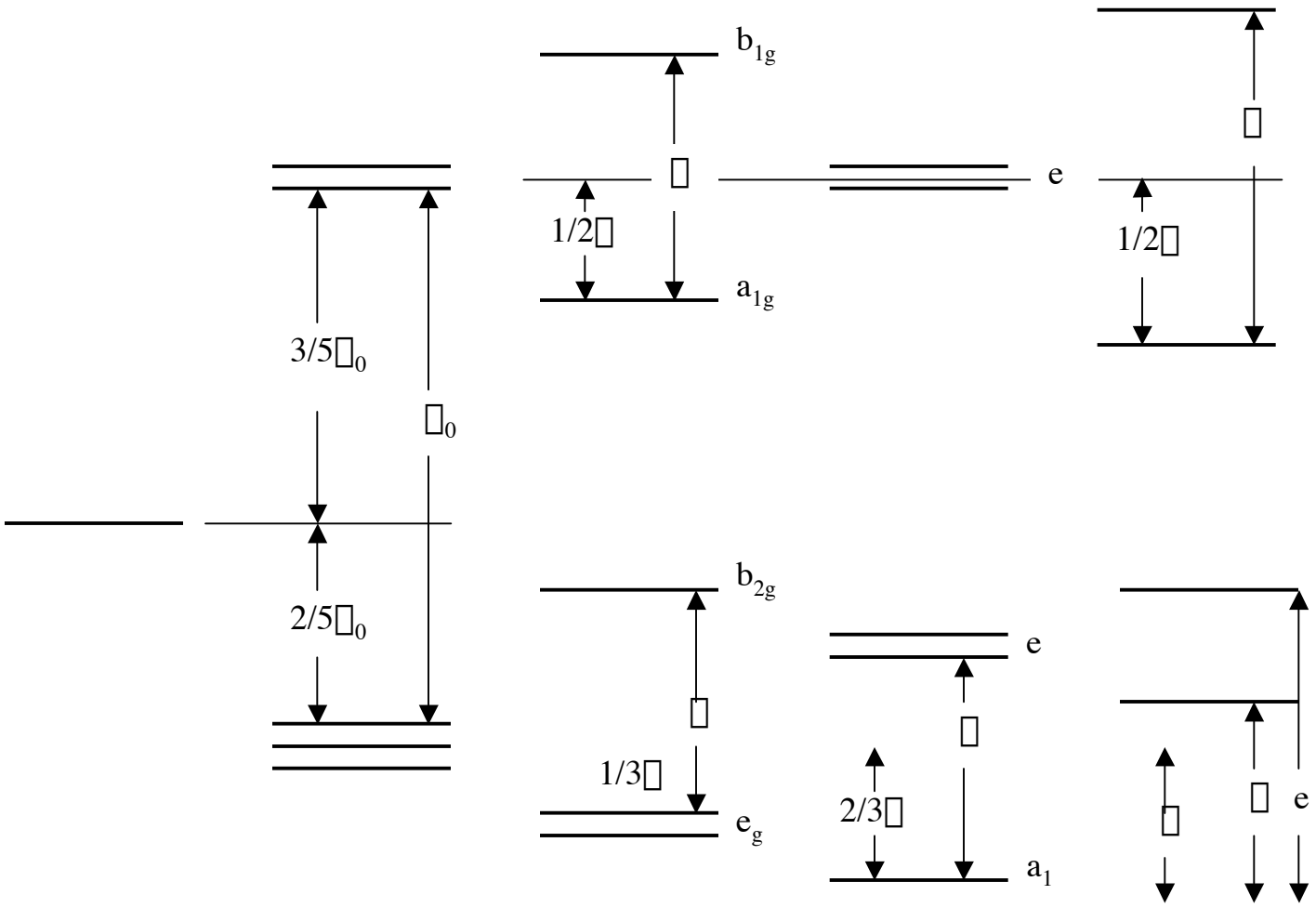


field-free ion | octahedral $O_h$ | tetragonal $D_{4h}$ | trigonal $C_{3v}$ | monoclinic $C_2$

As the site symmetry is reduced, the degeneracy of the one-electron energy levels is raised. For example, a tetragonal extension of the octahedron along the z-axis will lower $p_z$ and raise $p_x$ and $p_y$. The effect on the d-states is shown below. The degeneracy of the d-levels in different symmetry is shown in the table.

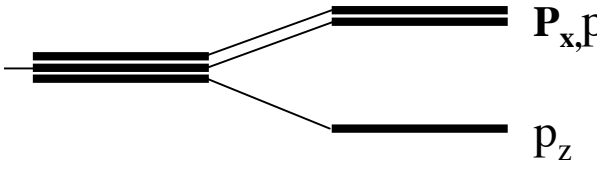


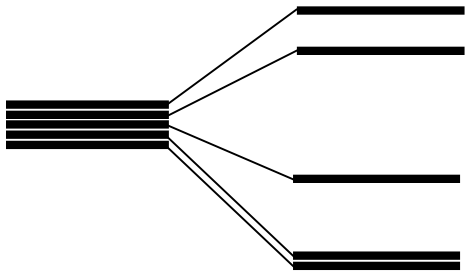

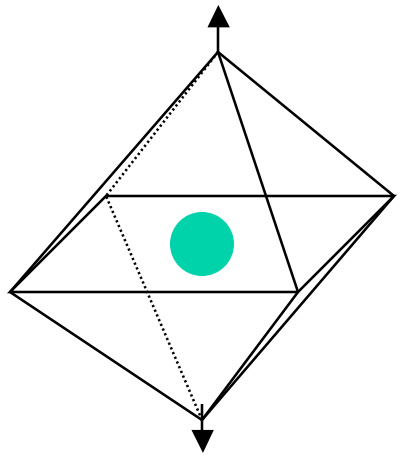

The effect of a tetragonal distortion of octahedral symmetry on the one-electron energy levels.

The splitting of the 1-electron levels in different symmetry

.

| | l | Cubic | Tetragonal | Trigonal | Rhombohedral |
|---|---|---|---|---|---|
| **s** | **1** | **1** | **1** | **1** | **1** |
| **p** | **2** | **3** | **1,2** | **1,2** | **1,1,1** |
| **d** | **3** | **2,3** | **1,1,1,2** | **1,2,2** | **1,1,1,1,1** |
| **f** | **4** | **1,3,3** | **1,1,1,2,2** | **1,1,1,2,2** | **1,1,1,1,1,1,1** |

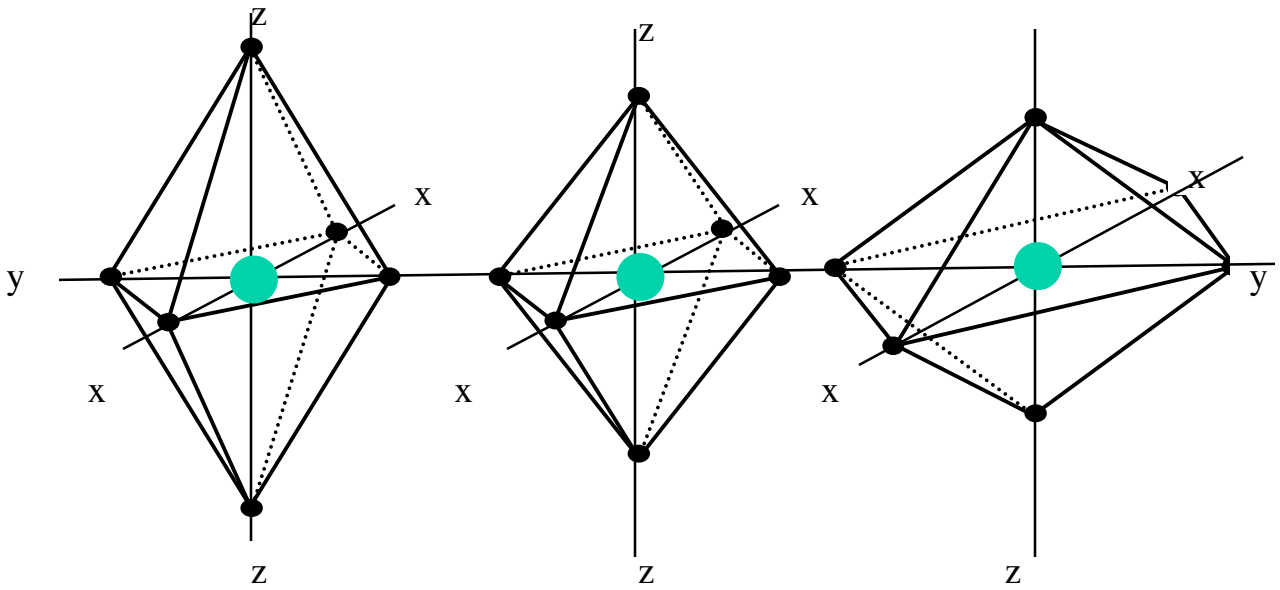


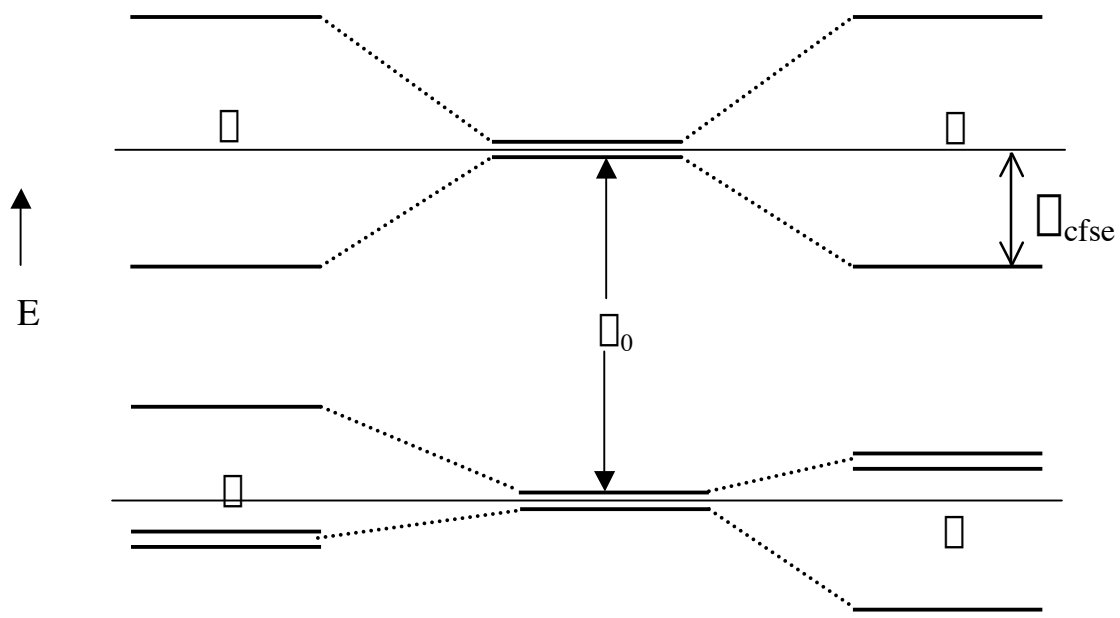


## Jahn Teller Effect

- A system with a single electron (or hole) in a degenerate level will tend to distort spontaneously. The effect is particularly strong for $d^4$ and $d^9$ ions in octahedral symmetry ($Mn^{3+}$, $Cu^{2+}$) which can lower their energy by distorting the crystal environment. This is the *Jahn-Teller* effect. If the local strain is $\varepsilon$, the energy change $\Delta E = -A\varepsilon + B\varepsilon^2$, where the first term is the crystal-field stabilization energy $\Delta_{cfse}$ and the second term is the increased elastic energy.

The J-T distorsion may be static or dynamic.

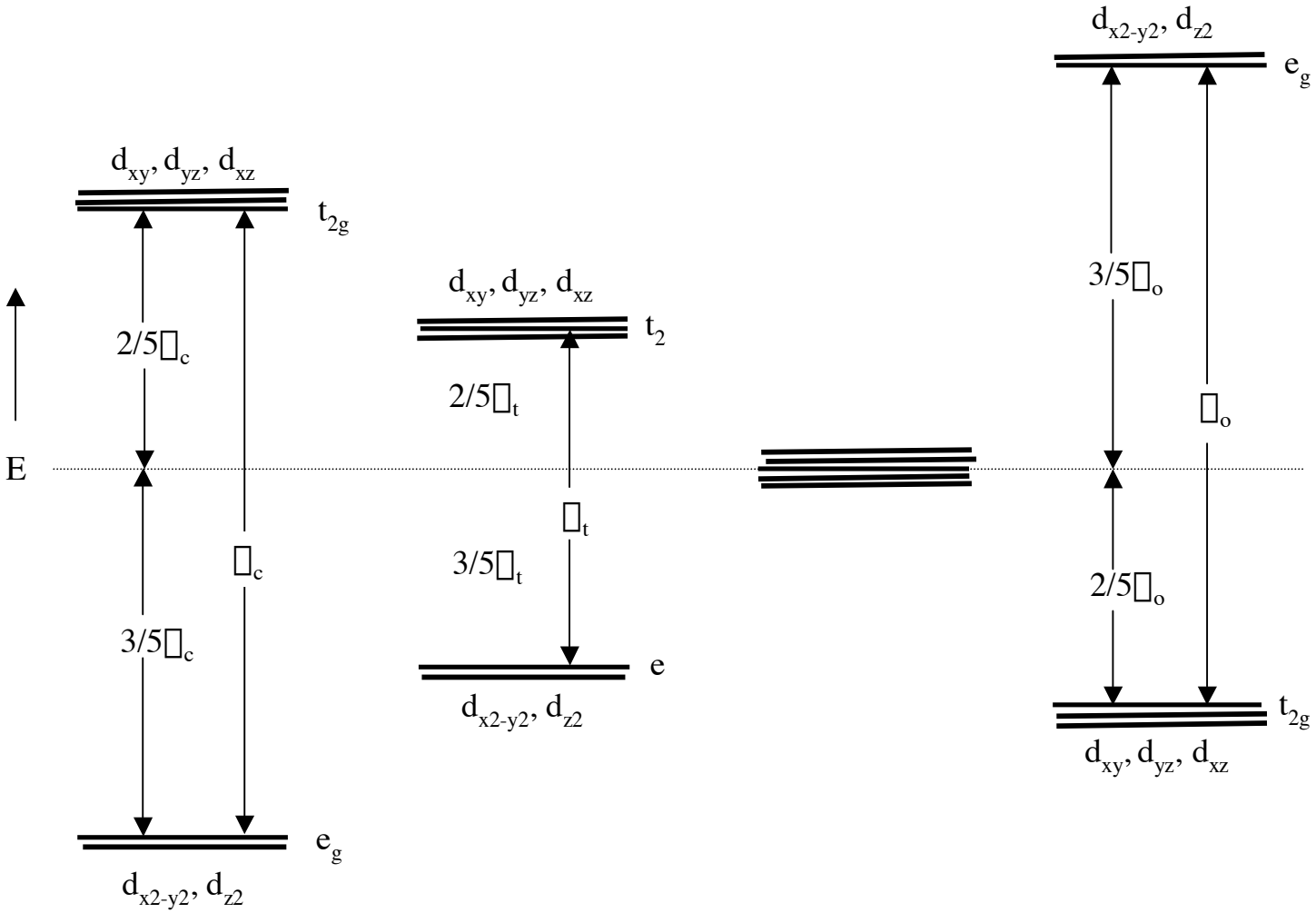
$d_{xy}, d_{yz}, d_{xz}$
$t_{2g}$
$2/5\Delta_c$
E
$\Delta_c$
$3/5\Delta_c$
$e_g$
$d_{x2-y2}, d_{z2}$
$d_{xy}, d_{yz}, d_{xz}$
$t_2$
$2/5\Delta_t$
$\Delta_t$
$3/5\Delta_t$
e
$d_{x2-y2}, d_{z2}$
$d_{x2-y2}, d_{z2}$
$e_g$
$3/5\Delta_o$
$\Delta_o$
$2/5\Delta_o$
$t_{2g}$
$d_{xy}, d_{yz}, d_{xz}$

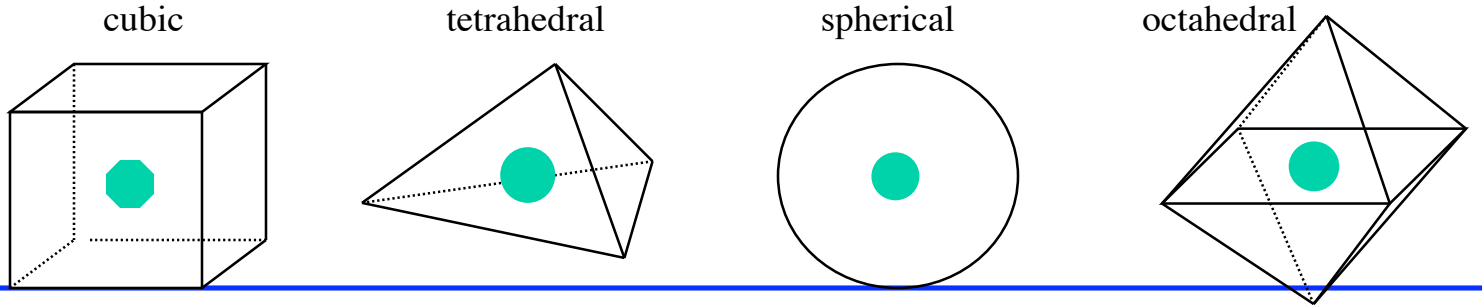
cubic
tetrahedral
spherical
octahedral

# 1.5.2 Multi-electron states

In insulators, the electrons in an unfilled shell interact strongly with each other giving rise to a series of sharp energy levels which are determined by the action of the crystal field on the orbital terms of the free atom. The spacing of theses levels may be determined by spectroscopy, and the crystal-field determined.

## Orgel Diagrams

These diagrams show the effect of a cubic crystal field on the Hund's rule ground state term. Since a half-filled shell has spherical symmetry, the cases $d^n$ and $d^{5+n}$ are equivalent. Also, since a hole is the absence of an electron, the cases $d^n$ and $d^{10-n}$ are related.

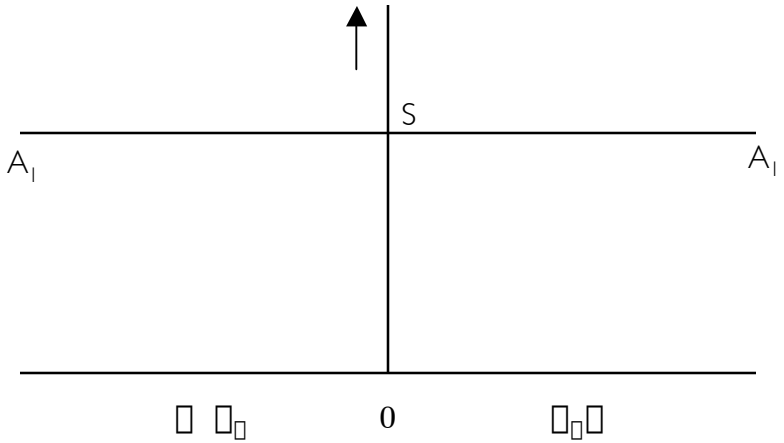


$d^5$ octahedral or tetrahedral

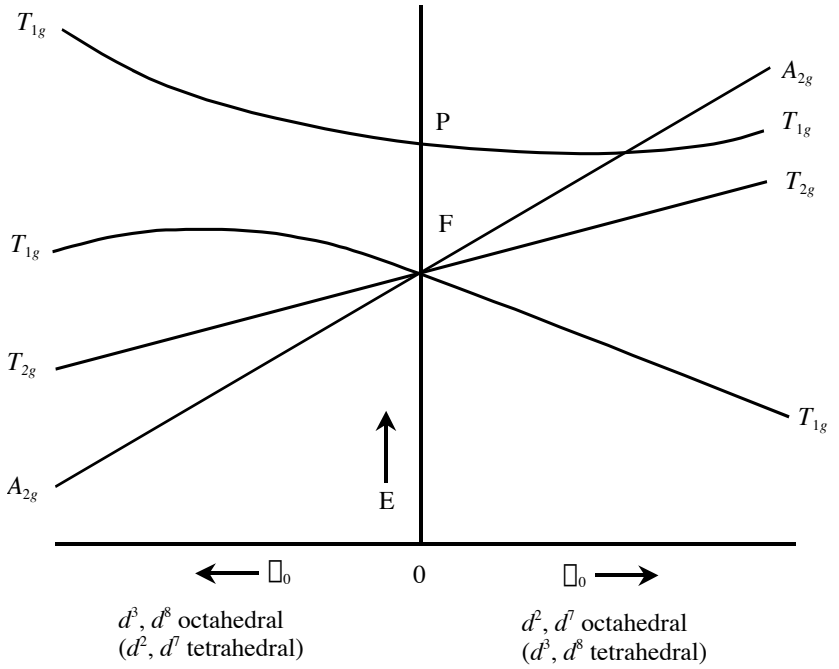


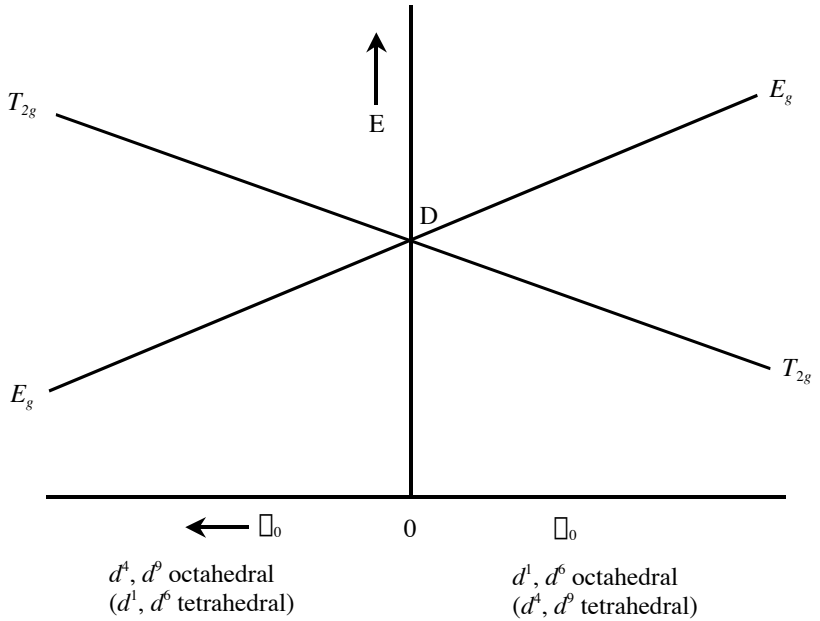

## High-spin and low-spin states

An ion is in a high-spin state or a low spin state, depending on whether the Coulomb interaction U leading to Hund's first rule (maximize S) is greater or less than the the crystal-field splitting □.

Consider a $3d^6$ ion such as $Fe^{3+}$.

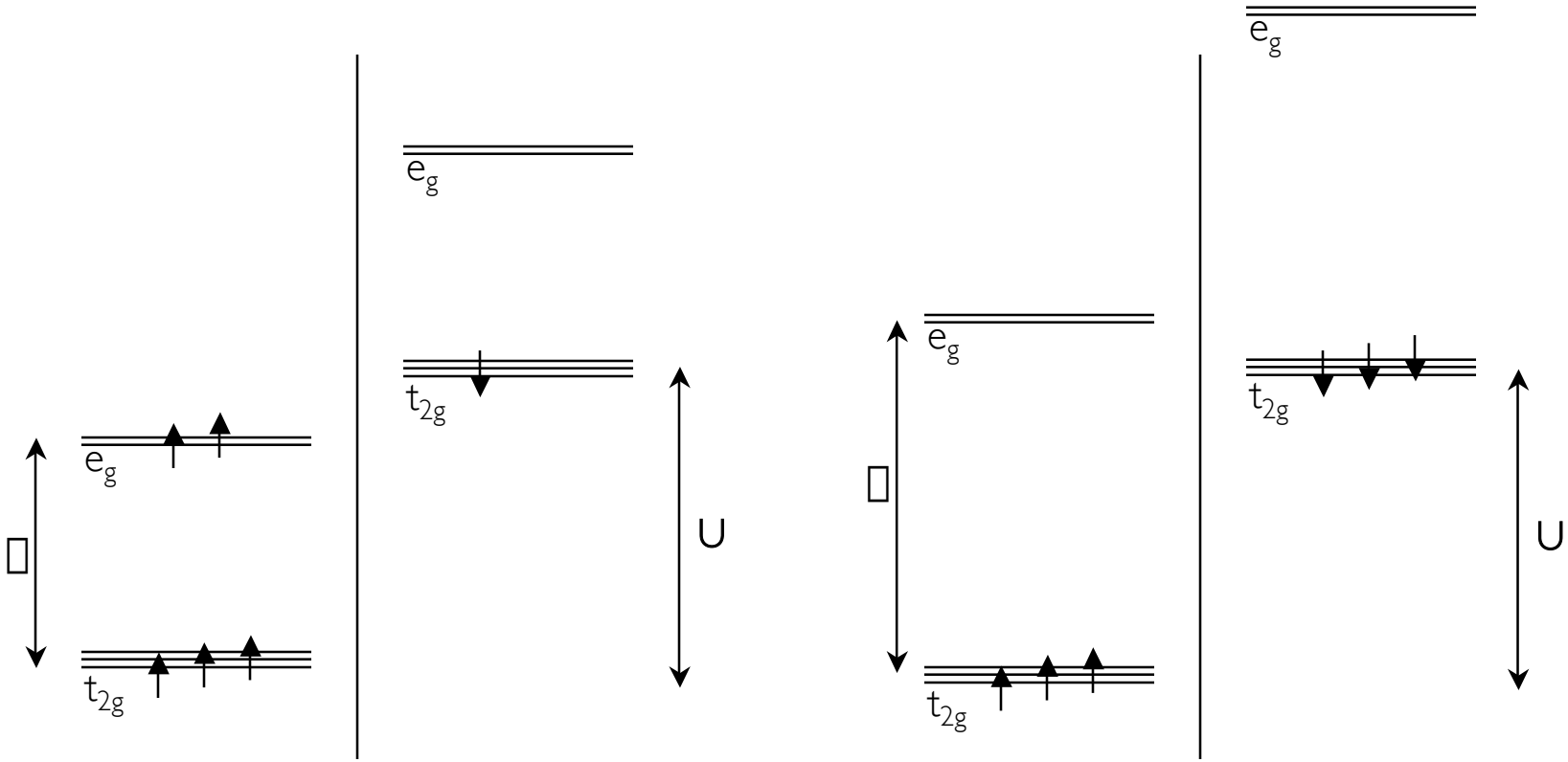


U > □, gives a high-spin state, S = 2 e.g. $FeCl_2$

U < □, gives a low-spin state, S = 0 e.g. Pyrite $FeS_2$

## Tanabe-Sugano diagrams

These show the splitting of the ground state and higher terms by the crystal field. The high-spin ⇄ low-spin crossover is seen. Diagrams shown are for d-ions octahedral environments.

### $d^6$

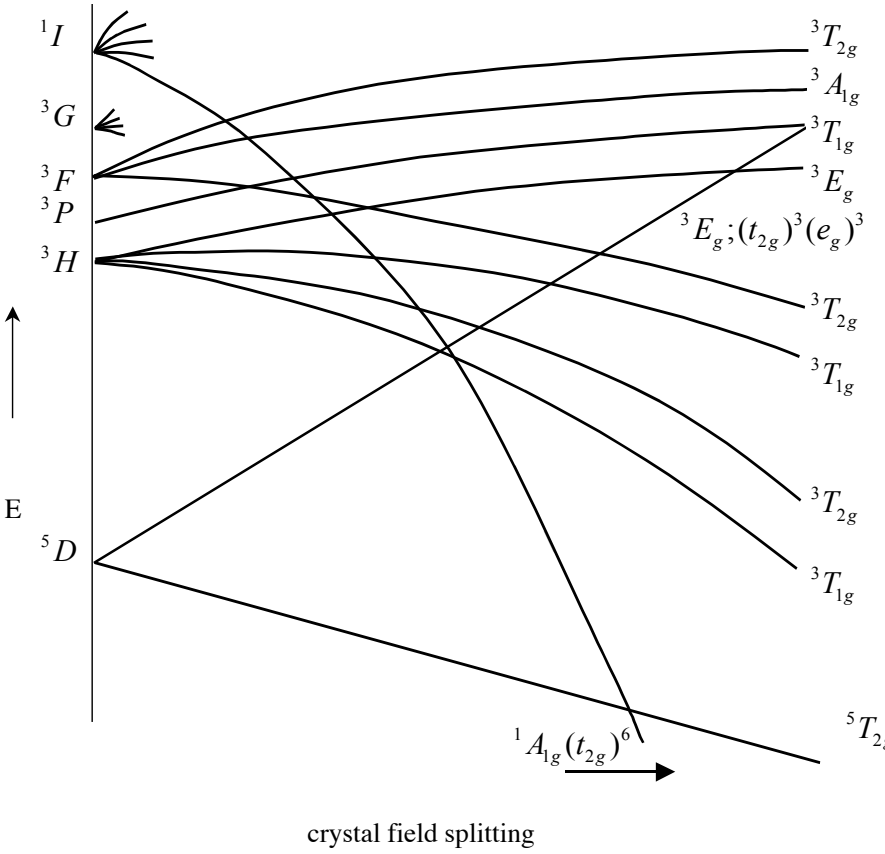


crystal field splitting

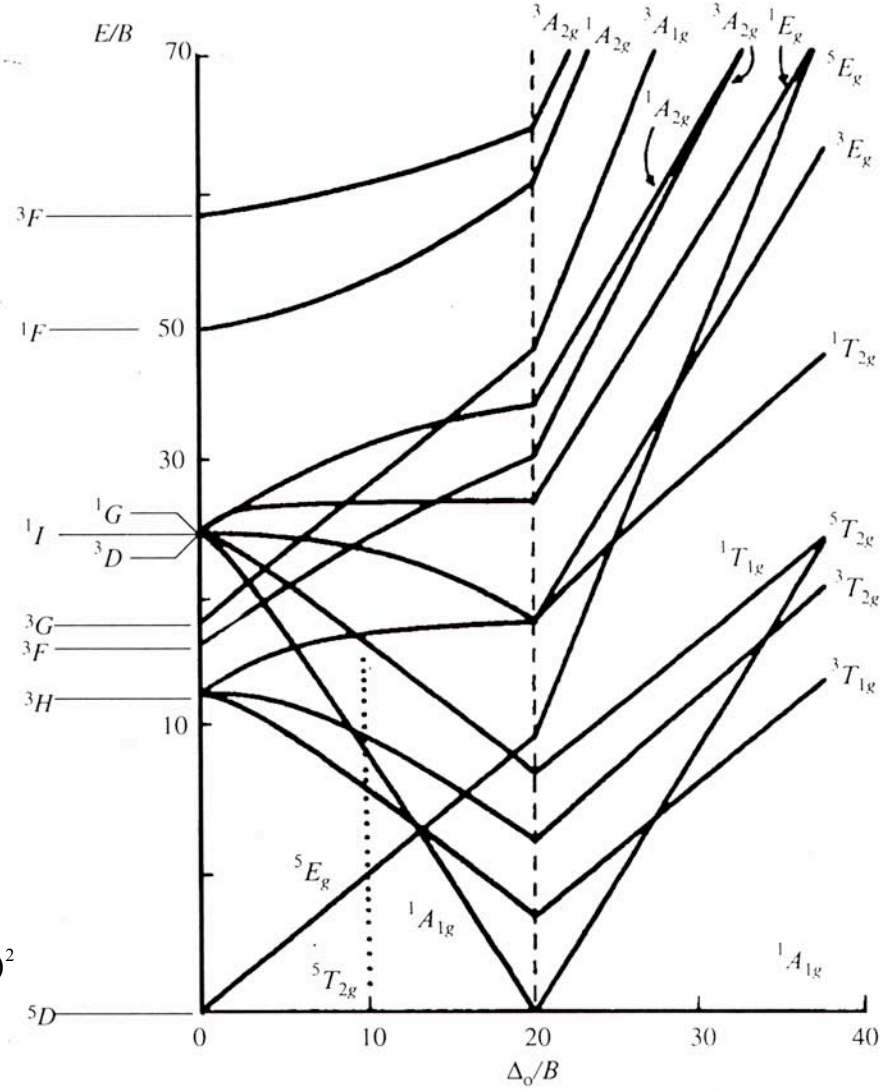

$d^5$

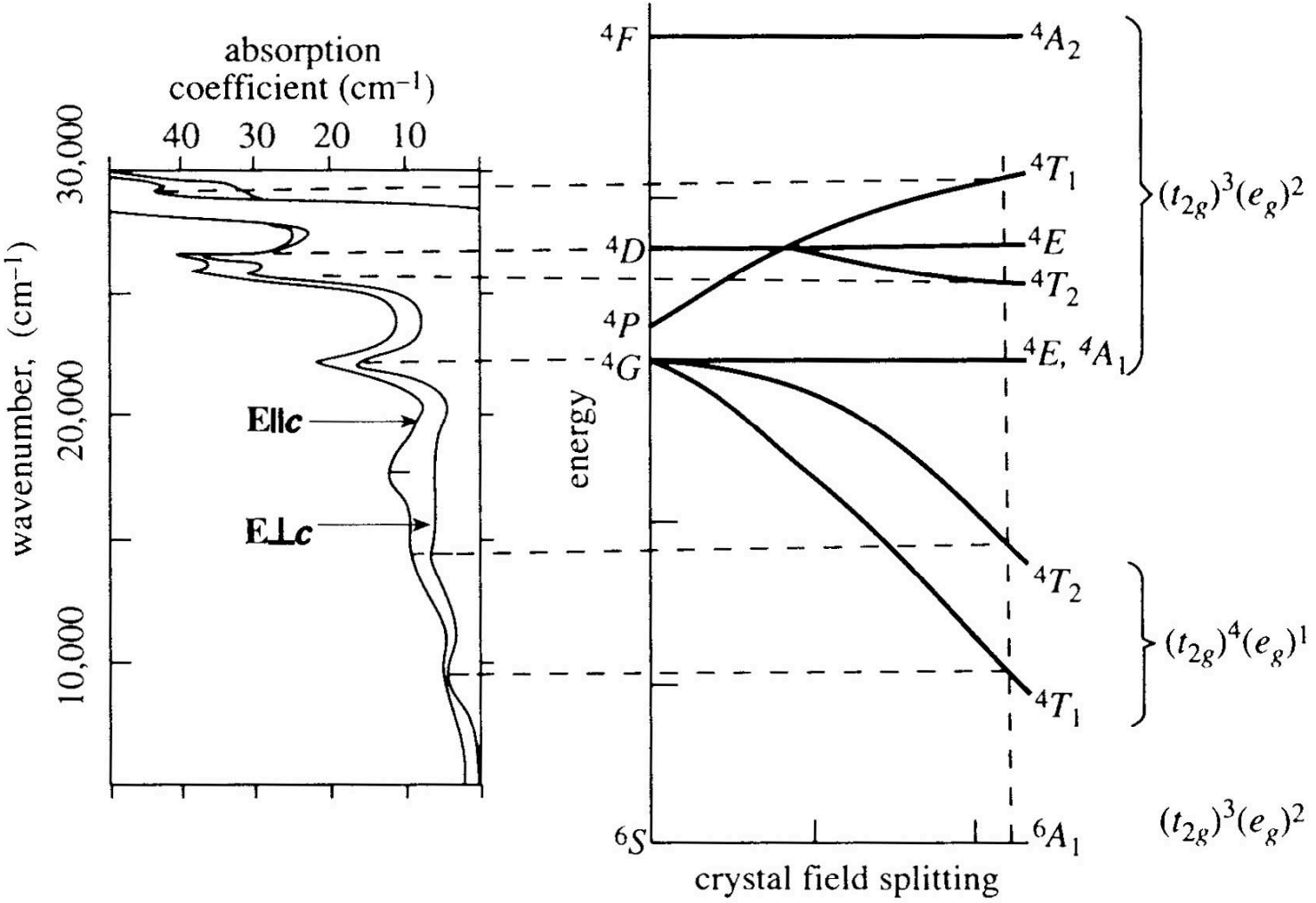


Matching the optical absorption spectrum of $Fe^{3+}$ - doped $Al_2O_3$ with the calculated Tanabe-Sugano energy-level diagram to determine the cubic crystal field splitting at octahedral sites.

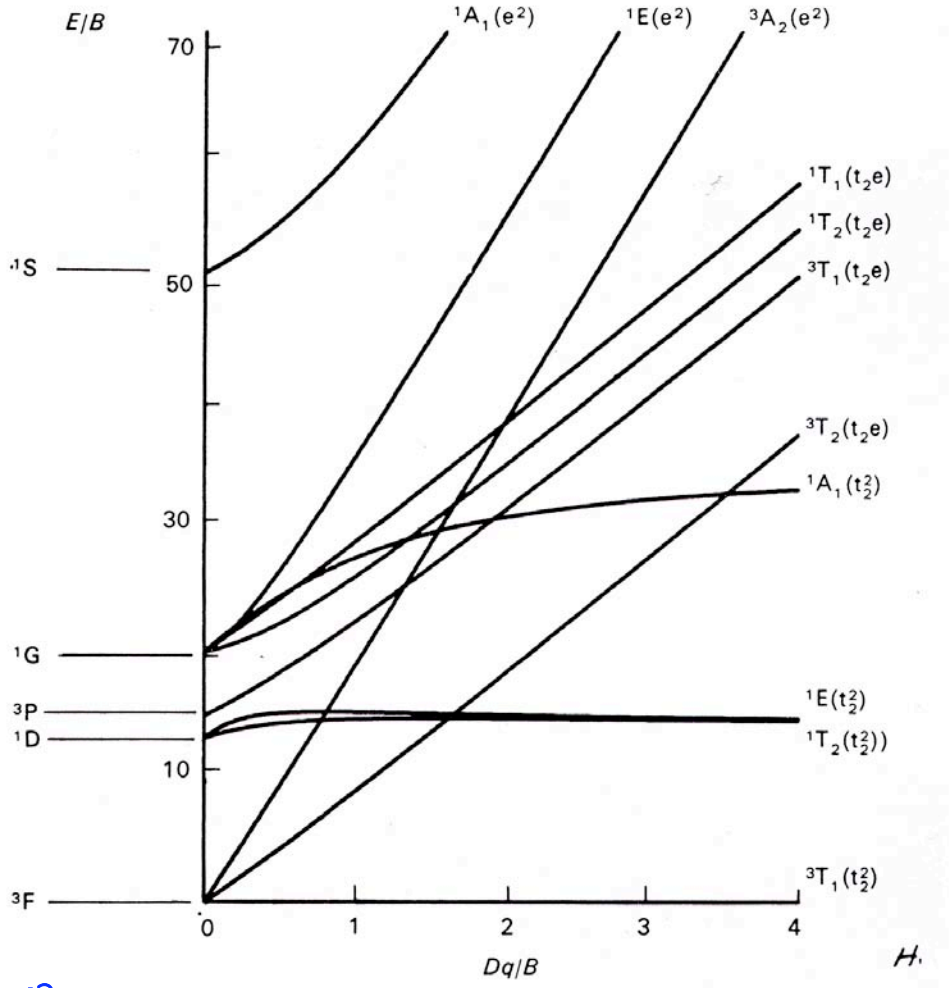


$d^2$

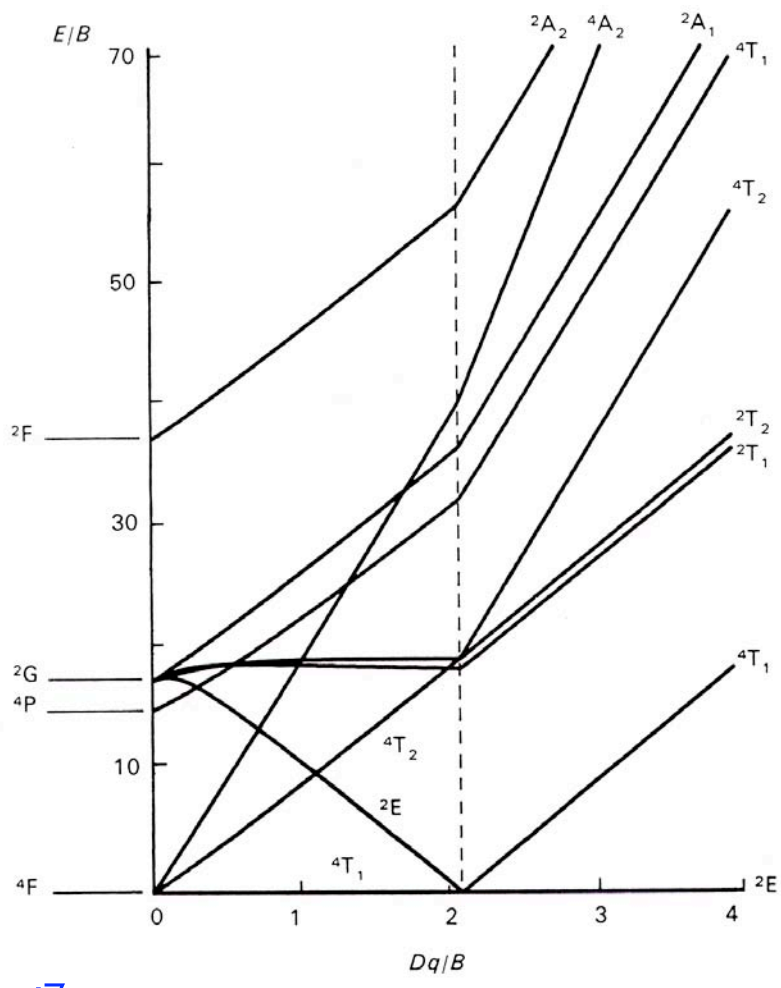


$d^7$

Note the similarities between the Tanabe-Sugano diagrams for $d^2$ and $d^7$. The differences are associated with the possible low-spin states for $d^7$ (e.g. $Co^{2+}$)

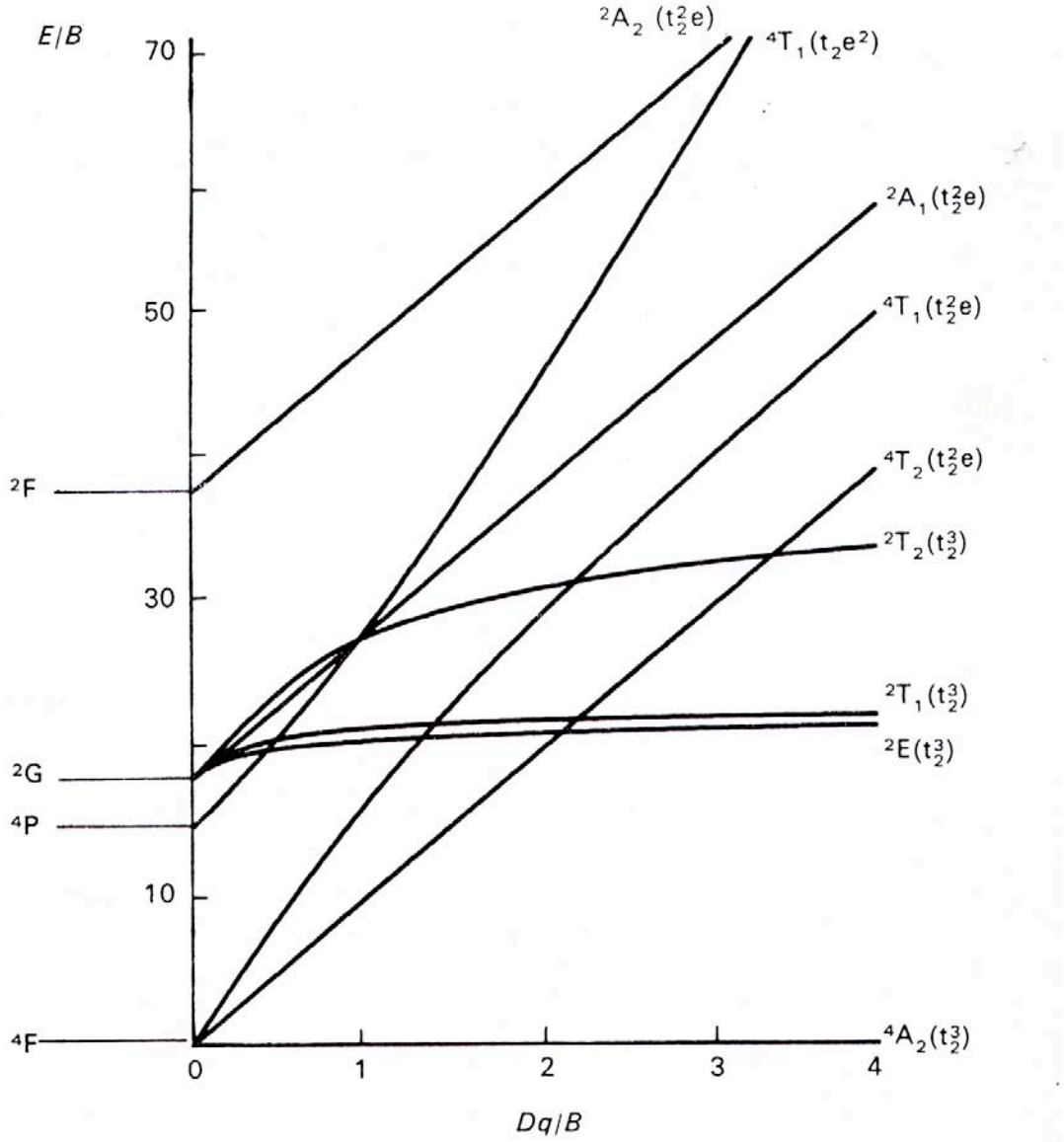


$d^3$

For $Cr^{3+}$ in $Al_2O_3$, the cf parameter Dq/B is 2.8

# 1.4 Crystal field and anisotropy

The electrostatic interaction of the ionic charge distribution $\rho(r)$ with the potential $V_{cf}$ created by the rest of the crystal gives rise to the crystal field splittings. It is also the source, via spin-orbit coupling, of *magnetocrystalline anisotropy*.

$$E = \int V_{cf}\,\rho(r)\,dr$$

where $$V_{cf}(r) = -(e/4\pi\varepsilon_0)\int\{\rho(R)/|R-r|\}\,dR$$

The anisotropy energy is therefore

$$E_a(r) = -(e/4\pi\varepsilon_0)\int\{\rho(r,\varepsilon)\,\rho(R)/|R-r|\}dr\,dR$$

Both the charge distribution $\rho(r)$ and the potential $V_{cf}(r)$ can be expanded in spherical harmonics.

Using the Wigner Eckart theorem, it is possible to write the corresponding crystal-field Hamiltonian in terms of angular momentum operators $J_x$, $J_{xy}$ $J_z$ $J^2$ which is a particularly useful way to find the energy-levels (eigenvalues). The Hamiltonian matrix is written in an $M_L$ or $M_J$ basis for the 3d transition elements or 4f rare earths respectively. In concise form

$$\mathcal{H}_{cf} = \sum_{n=2,4,6}\sum_{m=-n}^{n} B_n^m \hat{O}_n^m$$

Crystal field parameters

$B_n^m = \alpha_n \langle r^n \rangle A_n^m$

Stevens operators

Stevens coefficients

Crystal field coefficients

In a site with uniaxial anisotropy, the leading term is $\mathcal{H}_{cf} = B_2^0\,\hat{O}_2^0$ The Stevens operator $\hat{O}_2^0$ is $\{3J_z^2 - J(J+1)\}$

$$\mathcal{H}_{cf} = B_2^0\,\{3J_z^2 - J(J+1)\}$$

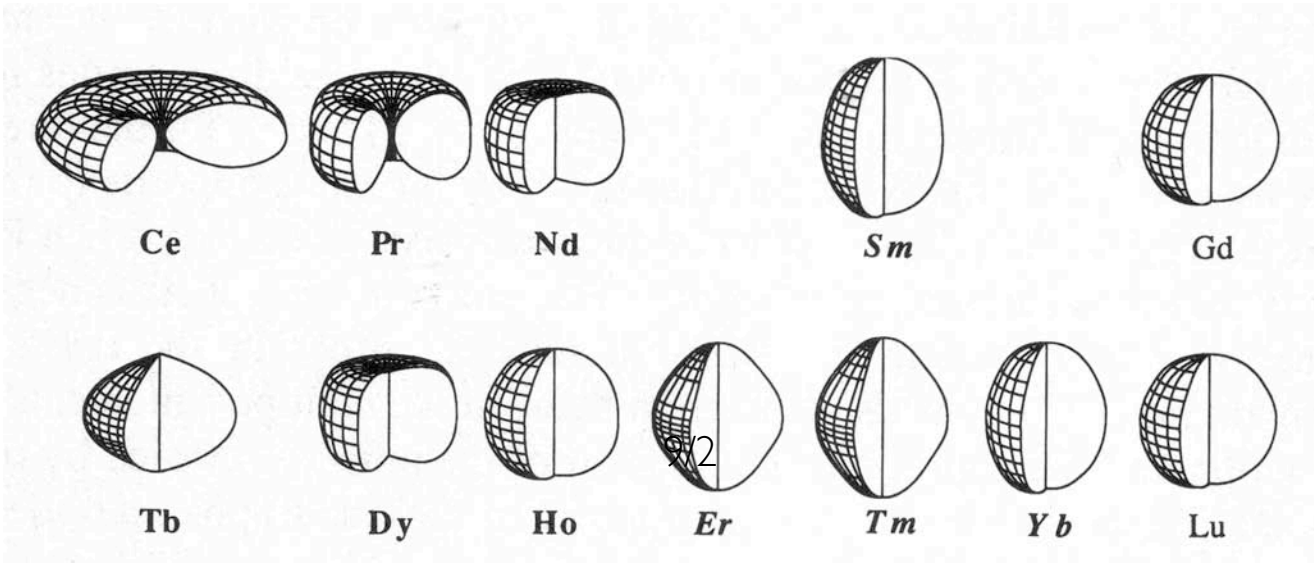


Charge distributions of the rare-earth ions. Those with a positive quadrupole moment ($Q_2 > 0$), italic type are distinguished from those with a negative quadrupole moment ($Q_2 < 0$) bold type. Note the quarter-shell changes,

e.g. $Nd^{3+}$ J = 9/2

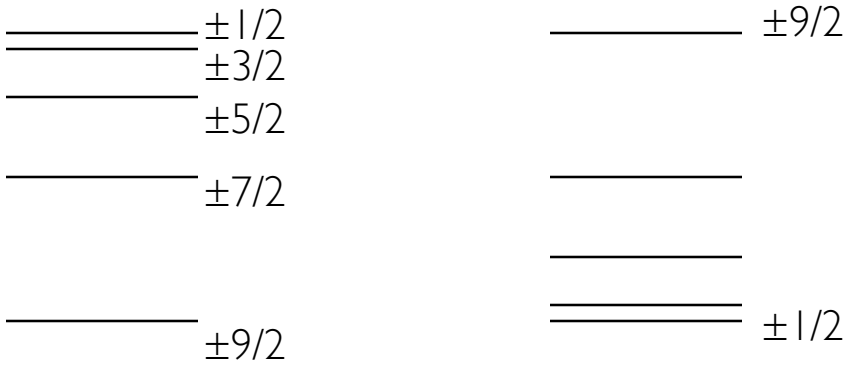


$B_2^0 < 0$ $B_2^0 > 0$